Diatom composition and fluxes over the Northwind Ridge, western Arctic Ocean: impact of marine surface circulation and sea ice distribution

Jian Ren, Jianfang Chen, Youcheng Bai, Marie-Alexandrine Sicre, Zhixiong Yao, Long Lin, Jingjing Zhang, Hongliang Li, Bin Wu, Haiyan Jin, et al.

Diatom composition and fluxes over the Northwind Ridge, western Arctic Ocean: impact of marine surface circulation and sea ice distribution

Jian Ren[a, b], Jianfang Chen[a, b, c*], Youcheng Bai[a, b], Marie-Alexandrine Sicre[d], Zhixiong Yao[b, c], Long Lin[b, c], Jingjing Zhang[a, b], Hongliang Li[a, b], Bin Wu[a, b], Haiyan Jin[a, b, c], Zhongqiang Ji[a, b], Yanpei Zhuang[a, b], Yangjie Li[a, b]

[a] *Key Laboratory of Marine Ecosystem Dynamics, Ministry of Natural Resources, Hangzhou 310012, China*

[b] *Second Institute of Oceanography, Ministry of Natural Resources, Hangzhou 310012, China*

[c] *State Key Laboratory of Satellite Ocean Environment Dynamics, Second Institute of Oceanography, Ministry of Natural Resources, Hangzhou 310012, China*

[d] *Sorbonne Université, Pierre et Marie Curie -CNRS-, LOCEAN Laboratory, 4 place Jussieu, F-75005 Paris, France*

[*] Corresponding author. E-mail: jfchen@sio.org.cn (Jianfang Chen)

Abstract

Over the last decades the western Arctic Ocean has undergone unprecedented environmental changes. However, long-term marine phytoplankton *in situ* observations are still rare and therefore insufficient to fully characterize evolutionary trends. This study investigate diatom flux and composition in sediment trap material collected in the Northwind Ridge, western Arctic Ocean from August 2008 to September 2009. Our data show that *Chaetoceros* resting spores are the predominant species accounting for >40% of the diatom composition. The sea ice diatom group, which includes *Fossula arctica*, *Fragilariopsis cylindrus* and *F. oceanica*, dominates the rest of the assemblage throughout the observation period. While the diatom fluxes in winter are extremely low, higher values are found in summer, with summer 2009 flux values being twice as high as in 2008. High total mass and diatom fluxes in summer 2009 are attributed to the intertwined effect of a weakened Beaufort Gyre, strengthened Pacific Water Inflow (PWI) and distribution pattern of the sea ice. Enhanced values of coastal diatoms and terrigenous proxies in summer 2009 are in agreement with intensified PWI. Sea ice diatoms and sea ice biomarker IP_{25} fluxes are both high during the sea ice melting season and significantly correlated ($r^2 = 0.64$, $p < 0.01$). Our data also suggest that sea ice diatoms are prone to selective dissolution in the water column and sediments, implying biases on diatom assemblages and subsequently on paleoceanographic reconstructions.

Key words: Diatoms, Sediment trap, Chukchi Sea, Northwind Ridge, Sea ice, Pacific water inflow, Beaufort Gyre

1. Introduction

Over the past decades, the Arctic Ocean has undergone unprecedented environmental changes with drastic impacts on the terrestrial (Post et al., 2013) and marine ecosystems (Carroll and Carroll, 2003; Grebmeier et al., 2006, 2012; Arrigo et al., 2008; Wassmann, 2011; Wassmann et al., 2011). Among other factors, the decline of sea ice has been shown to affect marine phytoplankton production and distribution patterns (e.g. Arrigo et al., 2008; McLaughlin et al., 2011; Coupel et al., 2012; Arrigo and van Dijken, 2015; Renaut et al., 2018). Blooms in autumn are now reported during the prolonged ice-free period in the Arctic (Ardyna et al., 2014) as well as significant changes in phytoplankton community due to enhanced freshening caused by global warming (Li et al., 2009; He et al., 2012; Coupel et al., 2015; Zhuang et al., 2018; Lee et al., 2019).

The highly productive Chukchi Sea in the western Arctic has experienced rapid sea ice retreat (Comiso, 2012; Serreze et al., 2016) leading to increased primary production and enhanced biological carbon uptake (Harada, 2016). The strengthening of the Pacific Water Inflow (PWI) bringing nutrients into the Chukchi Sea during the last decade (Woodgate et al., 2012; Woodgate, 2018) is another factor that may have altered the phytoplankton structure (Zhuang et al., 2016). The Chukchi Sea is thus a critical region for understanding oceanographic on-going and future changes in the Arctic Ocean and their consequences on polar ecosystems.

Apart from flagellates, diatoms appear to dominate the phytoplankton and bottom sea ice community in the Chukchi Sea (Booth and Horner, 1997; Sukhanova et al., 2009; Poulin et al., 2011; Joo et al., 2012). Because of diatom sensitivity to environment changes, their composition, abundance, distribution as well as size have been used as indicators of marine environmental conditions (Zernova et al., 2000; Smol and Stoermer, 2010; Romero and Armand, 2010). For instance, recent studies speculated that the occurrence of the endemic North Pacific diatom *Neodenticula seminae* in the North Atlantic might reflect stronger PWI driven by sea ice loss (Reid et al., 2007; Poulin et al., 2010; Bluhm et al., 2011). Better understanding of the relationship between diatoms and environmental variables today is also essential to produce robust paleoceanographic reconstructions based on fossil diatoms in Arctic sediments (e.g. Ren et al., 2009; Sha et al., 2016, 2017; Miettinen, 2018). Paleo-records are still very sparse in the western Arctic in part because of our poor knowledge of modern diatom ecology and the complex deposition pathways in this environment.

Sediment traps have been extensively deployed throughout the world ocean to study biological processes and carbon export (Romero and Armand, 2010). In the Arctic, sediment trap deployments have focused on the continental shelves and slopes (e.g. Wassmann et al., 2004 and references therein; O'Brien et al, 2006, 2011; Fahl and Nöthig, 2007; Forest et al.,

2007, 2008, 2011; Lalande et al., 2009; Fahl and Stein, 2012) as well as the deep basins (Honjo et al., 2010; Hwang et al., 2015; Lalande et al., 2019). Few studies have been undertaken in the Chukchi Sea. Analyses of the ice-tethered sediment traps over the Chukchi Rise revealed the heterogeneous patterns of biological processes and variety of particulate organic carbon sources (Honjo et al., 2010). Recent studies of the first multi-years mooring observations in the Northwind Abyssal Plain have documented seasonal variations of phyto- and zooplankton (Matsuno et al., 2014; Ikenoue et al., 2015; Onodera et al., 2015, 2016; Tokuhiro et al., 2019) and also evidenced early winter high flux induced by cold eddies from the shelf-break (Watanabe et al., 2014, 2015).

In this study, we report on seasonal variations of diatom vertical flux obtained from the sediment trap mooring deployed over the Northwind Ridge, Chukchi Borderland from August 2008 to September 2009 as part of the Chinese National Arctic Research Expedition (CHINARE) program. These data are compared to the biomarker data of Bai et al. (2019) measured in the same samples and discussed in light of the overlying water mass characteristics, sea ice concentrations and atmospheric circulation in the western Arctic Ocean.

2. Oceanographic settings

Station DM is located at the southern Northwind Ridge, a steep ledge extending from the shallow Chukchi Shelf into the Arctic deep basin as a part of the Chukchi Borderland (Fig. 1). The surface hydrology of the region is influenced by the dynamic Beaufort Gyre (BG) circulation, the PWI entering the Arctic Ocean through the Bering Strait and the seasonal sea ice coverage.

The anticyclonic BG circulation is driven by the Beaufort High (Proshutinksy and Johnson, 1997). Over the last two decades, the stronger BG circulation has resulted in enhanced freshening in the Canadian Basin (Giles et al., 2012) with significant impact on the phytoplankton productivity and polar ecosystem (He et al., 2012; Coupel et al., 2015).

The PWI is primarily driven by a sea level difference between the Bering and Chukchi Seas (Coachman and Aagaard, 1966), leading to an average northward water transport of ~0.8 Sv (Roach et al., 1995). The PWI splits into three water masses in the Chukchi Sea, i.e. the saline and nutrient-rich Anadyr Water (AW) as the western branch, the fresher and nutrient-depleted Alaska Coastal Water (ACW) to the East, and in between the Bering Shelf Water (BSW) of intermediate salinity (Fig. 1; Woodgate et al., 2005a; Grebmeier et al., 2006). In the past two decades, long-term mooring observations in the Bering Strait have shown a gradual increase of the PWI volume transport (~70% from 2001 to 2014; Woodgate et al., 2012; Woodgate, 2018), entraining more heat and nutrients into the Arctic Ocean. In the western Chukchi Sea, the fresher Siberian Coastal Current (SCC) periodically interacts with the AW.

Sea ice occurs in the study area from November to July while it reaches a minimum over the northern Chukchi Sea in September (Fig. 1). Several studies have shown that sea ice reduction induced by PWI impacts on marine ecosystem (e.g. Shimada et al., 2006; Harada, 2016; Serreze et al., 2016). It has also been hypothesized that sea ice motion is also correlated, at least partially, with the Arctic Oscillation (AO) (Rigor et al, 2002; Shimada et al., 2006).

3. Material and methods

3.1 Sediment trap samples

A one year-round mooring was deployed at Station DM (DM hereafter) on the southern Northwind Ridge, in the vicinity of the Canada Basin, from August 2008 to September 2009 (Fig. 1; 74°24.0' N, 158°14.0' W, 1650 m water depth). This conical sediment trap (McLane PARFLUX Mark 78H-21) was equipped with 21 sampling cups and installed at ~870 m water depth. Samples were generally collected every two weeks (15 or 16 days, depending on the month) during the diatom production season (July to November) while during the low flux period in winter (December to June) sampling intervals were longer (28 to 31 days, depending on the month; Bai et al., 2019). The 21 sampling cups were filled with artificial seawater (salinity≈35) and antiseptic $HgCl_2$ to preserve trap material from degradation.

After recovery, the wet samples were sieved using a 1-mm mesh nylon sieve to remove swimmers. The fine fractions (<1 mm) were split into aliquots with a McLane wet sample divider (WSD-10). An aliquot (1/4 or 1/8) was filtered on a polycarbonate filter (0.45 μm pore size, 47 mm diameter) for diatom and biochemical analyses. Samples were then dried in an oven at 45 °C for 72 h (Bai et al., 2019).

3.2 Diatom preparation and analysis

Quantitative diatom slides were prepared according to the standard method developed at the Alfred Wegener Institute, Germany (Gersonde and Zielinski, 2000). For each cup, 30 mg or 15 mg sub-sample was used. Although only 1 mg was available for cup 14# (May 2009), the sample was analyzed to keep the entire record intact. The subsamples were then treated with HCl (~36% w/w concentration) and H_2O_2 (~30% w/w concentration) to remove calcareous and organic material. After rinsing, a known aliquot of the residue was evenly dropped on a cover glass (24 mm × 24 mm). Permanent slides were mounted with Naphrax for diatom identification (n_D ~1.7; Fleming, 1954).

Around 400 diatom valves (max. 604.5, min. 372) were counted for each sample with a Motic BA400E microscope at ×1000 magnification. For cup 14# only 215 diatom valves could be counted. Diatom valves were counted according to the method of Schrader and Gersonde (1978). Diatoms were identified to species level following Medlin and Priddle (1990), Hasle

and Syvertsen (1997), Suto et al. (2004), Katsuki et al. (2009), Obrezkova et al. (2014) and Tsoy and Obrezkova (2017). Because resting spores of genus *Chaetoceros* can hardly be identified at a species level by light microscopy, they were combined and labeled as *Chaetoceros* resting spores (RS).

The diatom counts were converted into relative abundances with respect to the total diatom assemblage. The diatom concentration (valves per gram dry sample) was estimated using the following formula (Esper et al., 2010):

$$Diatom\ concentration = (1/dw) \times (csa/ta) \times (sv/split) \times (vn/tn) \quad (1)$$

in which, *dw* is the dried sample weight in milligrams, *csa* is the area of the cover slide (576 mm^2), *ta* is the area of one counted traverse (6 mm^2), *sv* is the volume of processed diatom suspension (6-15 ml), *split* is the volume of aliquot dropped onto the cover slide (from 27 to 81 $\times 10^{-2}$ ml), *vn* is the total counted diatom valves and the *tn* is the number of fully counted traverses.

The diatom fluxes were calculated by the following equation:

$$Diatom\ flux\ [valves\ m^{-2}\ d^{-1}] = Total\ mass\ flux\ [mg\ m^{-2}\ d^{-1}] \times Diatom\ concentration\ [valves\ mg^{-1}] \quad (2)$$

where the diatom concentration is derived from equation (1).

Diatom taxonomic diversity was evaluated by the H-index based on the Shannon-Weaver formula (Shannon and Weaver, 1949):

$$H = -\Sigma P_i \log_2 P_i \quad (3)$$

where H is the diversity index and P_i is the relative abundance of species i.

3.3 Biomarker analysis

The concentrations of IP_{25} and brassicasterol (24-methylcholesta-5,22E-dien-3β-ol) published by Bai et al. (2019) are used for comparison with our diatoms fluxes to discuss sea ice conditions. Campesterol (24-methylcholest-5-en-β-ol) and 24-ethylcholest-5-en-3β-ol are also used to assess higher plant inputs. All sterols were silylated with 100 μL BSTFA (bis-trimethylsilyl-trifluoroacet-amide) (80 °C, 1 h) prior to the gas chromatography (GC) analysis. The GC analyses were carried out on a Varian 3300 with a septum programmable injector and a flame ionization detector (Bai et al., 2019).

3.4 Carbonate and lithogenic matter

The $CaCO_3$ content of sinking material was calculated from particulate inorganic carbon (PIC) values determined by the difference between total carbon (TC) and particulate organic

carbon (POC; Bai et al., 2019). The lithogenic matter (LM) was estimated as the difference between the total mass (TM; from Bai et al., 2019) and the biogenic material composed of $CaCO_3$, opal (Wu et al., unpublished data) and organic matter (OM) that conventionally convert from POC by a factor of 1.8 (Müller et al., 1986):

$$LM = TM - (CaCO_3 + Opal + OM) \quad (4)$$

The lithogenic matter percentage was then calculated by the following equation:

$$LM\ (\%) = LM/TM \quad (5)$$

3.5 Environmental data

Daily environmental data over the study period at DM, including shortwave radiation, snow thickness, sea ice cover and sea ice thickness, were from the National Centers for Environmental Prediction (NCEP)/Climate Forecast System Reanalysis (CFSR) 6-hourly dataset (Saha et al., 2010, 2014).

Monthly Pacific inflow data, e.g. volume transport, temperature and salinity, were acquired from the "Bering Strait: Pacific Gateway to the Arctic" project (Woodgate et al., 2015; Woodgate, 2018).

Regional sea ice concentrations were from Nimbus-7 SMMR and DMSP SSM/I-SSMIS Passive Microwave Data with a grid resolution of 25 × 25 km (Cavalieri et al., 1996).

Summer (July, August, September) monthly averaged sea surface chlorophyll-*a* concentrations for a 2° × 2° area around DM were retrieved from the Moderate Resolution Imaging Spectroradiometer (MODIS) with a 4 × 4 km resolution and calculated by algorithm of Gohin et al (2002) collected by GlobColour data (http://globcolour.info).

4. Results

4.1 Environmental conditions

Station DM experiences polar night from November to mid-February and receives maximum solar irradiance of ~369 W m^{-2} in summer, from mi-April to mid-July (Fig. 2a). Seasonal sea ice was present from late October 2008 to mid-August 2009. The ice-free season (sea ice concentration <15%) is approximately one month longer in 2008 than in 2009 (mid-July to late October vs. mid-August to early October, respectively; Fig. 2b). Winter sea ice thickness over the station is 2.19 m on average with a maximum thickness of 2.79 m recorded in March 2009 (Fig. 2c). Similarly, snow on ice appears in mid-October 2008 and nearly has thawed out early June 2009 (Fig. 2d). The snow accumulation is over 25 cm in winter.

4.2 Total mass flux

The seasonal pattern of the total mass fluxes (TMF) earlier described by Bai et al. (2019), show higher values in August and September, both in 2008 and 2009 (Fig. 2e). However, the TMF in September 2009 is ca. eightfold larger than in 2008. Particulate organic carbon (POC) fluxes exhibit similar fluctuations as TMF, with extremely low values in winter and early spring, from November 2008 to June 2009 (Fig. 2f). One exception to this is the POC flux value of 3.51 mg m^{-2} d^{-1} in April 2009, representing approximately 12% of the TMF as compared to an annual mean value of 4% (Bai et al., 2019).

4.3 Lithogenic matter flux

In few samples, the PIC content is negative as a result of POC values exceeding the TC values (PIC = TC - POC). These numbers reflect the very low PIC content of these samples (<1%), and uncertainties on TC and POC measurements. Thus the $CaCO_3$ contents based on these PIC values became negative. In general, $CaCO_3$ is less than 10% of the total mass and has thus no significant impact on the lithogenic matter content. Accordingly, we revised the negative carbonate values to zero. The derived lithogenic matter fluxes reach 225 mg m^{-2} d^{-1} and ~600 mg m^{-2} d^{-1} in summer of 2008 and 2009, respectively, while low values (<50 mg m^{-2} d^{-1}) are recorded in winter (Fig. 2e). On average, the lithogenic matter accounts for >70% of the total mass with no clear seasonal pattern (Fig. 2e).

4.4 Terrigenous sterol flux

Fluxes of 24-ethylcholest-5-en-3β-ol show similar variations as terrigenous campesterol suggesting a primary terrestrial source of this sterol, thus most likely mainly represented by β-sitosterol (Fig. 2g). Campesterol and β-sitosterol fluxes reach ~1 and 2.8 μg m^{-2} d^{-1} in August 2008, respectively. Both decrease to less than 0.5 μg m^{-2} d^{-1} in the following winter (Fig. 2g) and increase to highest fluxes in summer 2009 peaking at 9.6 μg m^{-2} d^{-1} in July for β-sitosterol, and to 8.4 μg m^{-2} d^{-1} in September for campesterol.

4.5 Diatom flux and species composition

Total diatom fluxes are strongly seasonal (Fig. 2h). Two peak values occur early August 2008 (~10×10^6 valves m^{-2} d^{-1}) and late July to September 2009 (>14×10^6 valves m^{-2} d^{-1}), respectively. The diatom fluxes in winter are two orders of magnitude lower (<0.5×10^6 valves m^{-2} d^{-1}). They rise abruptly late July 2019 when solar irradiance is nearly at maximum and sea ice starts retreating (Fig. 2a, b, h).

In total 93 diatom species or species groups were identified in the sediment trap samples. Apart from *Chaetoceros* RS, diatoms were categorized into 4 groups based on their ecological preferences (Medlin and Priddle, 1990; Hasle and Syvertsen, 1997; von Quillfeldt, 1997, 2000; Kohly, 1998; von Quillfeldt et al., 2003; Onodera et al., 2015). The sea ice group mainly

consists of *Fossula arctica*, *Fragilariopsis cylindrus*, *F. oceanica*, *Nitzschia frigida*, *Pauliella taeniata* and certain species of genera *Diploneis*, *Navicula*, *Nitzschia*, *Pinnularia*. The cold-water diatom group is mostly composed of *Thalassiosira antarctica* var. *borealis* RS, *T. nordenskioeldii* and, in minor amounts, *Bacterosira bathyomphala* RS and *T. bulbosa*. The cosmopolitan diatom group includes *Chaetoceros atlanticus*, *Thalassionema nitzschioides* and *Thalassiosira eccentrica*, while *Paralia sulcata* and species of genera *Cocconeis*, *Cyclotella*, *Cymbella*, *Delphineis* and *Eunotia* form the coastal diatom group. The remaining diatom species make up the other group.

Chaetoceros RS is the predominant group over the entire observation period (Fig. 3a). It increases from 40% in August 2008 to ~80% in late September 2009. In contrast, the sea ice diatom group shows a broad decline since the deployment of the trap (Fig. 3b-e). Within this group, the relative abundances of *F. arctica*, *F. cylindrus* and *F. oceanica* are two- to three-fold higher in summer 2008 than in 2009, whereas *P. taeniata* peaks in November 2008. The cold-water diatom group, however, remains low throughout the study period (Fig. 3f-g). Unlike the sea ice diatom species, the cold-water *T. antarctica* var. *borealis* RS, *T. bulbosa* and *T. nordenskioeldii* are more abundant in summer 2009 than in summer 2008. Interestingly, *T. nitzschioides*, the major representative of the cosmopolitan diatom group, is more frequently observed in winter than in summer (Fig. 3h). Similarly, the coastal diatom group, dominated by *P. sulcata*, is also found in low relative abundances with slightly higher values from October 2008 to April 2009 when sea ice prevails (Fig. 3i).

Among the sea ice diatoms, *Haslea crucigeroides* and *Pleurosigma stuxbergii* var. *rhomboides*, that are known producers of sea ice biomarker C_{25} monounsaturated hydrocarbon IP_{25} (Brown et al., 2014), are detected though in low relative abundance (<1%), in both August 2008 after sea ice just retreated, and in July - early August 2009 at the onset of sea ice thaw (not shown). Although widely observed in the Arctic Ocean, the sea ice bottom tethered diatom *Melosira arctica* is only found sporadically over this one-year experiment (Abelmann, 1992; Zernova et al., 2000; von Quillfeldt et al., 2003; Boetius et al., 2013; Lalande et al., 2014, 2019).

The North Pacific predominant and endemic taxa *Neodenticula seminae* (Jousé et al., 1971; Sancetta, 1982; Onodera and Takahashi, 2009; Ren et al., 2014), which has been recently reported in the North Atlantic water column and surface sediment (Starr et al., 2002; Reid et al., 2007; Miettinen et al., 2013), is also found once in sinking particles at DM, in line with the data obtained at the nearby sediment trap NAP site (Onodera et al., 2015).

4.6 Diatom taxonomic diversity

The diatom diversity index, H-index, decreases from a mean of ~2.6 in 2008 to ~2.3 in 2009 with an outlier value of ~3.9 in early July 2009 (Fig. 3j). The summer 2009 diversity minimum

is reached at maximum TMF and diatom fluxes (Fig. 2e, h, 3j). The H-index of summer 2009 is lower than found in summer 2008 (H-index: 1.8 vs 2.7) most probably due to the high abundance of *Chaetoceros* RS and decrease of other species.

5. Discussion

5.1 Interannual variability of diatom fluxes: link to surface circulation and sea ice

Our sediment trap time-series shows high TMF and diatom flux values during the summer season. However, in summer 2009 and particularly late September, fluxes are two- to three-fold higher than measured in 2008 (Fig. 2e, h; Bai et al., 2019). Diatom fluxes in summer 2008 (~10×10^6 valves m^{-2} d^{-1}) are comparable to those found during the same season in the nearby station NAP at 180/260 m depth in 2011 (~11×10^6 valves m^{-2} d^{-1}), regardless of the mooring depths and collection years of each site (Onodera et al., 2015). Interestingly, the high diatom flux values in summer 2009 at DM (14 to 27×10^6 valves m^{-2} d^{-1}) are of similar magnitude as winter high flux events at NAP attributed to shelf-break eddies (Watanabe et al., 2014; Onodera et al., 2015).

Lower diatom fluxes in 2008 than 2009 may suggest that the summer bloom was not captured (Fig. 2-3) and that these low values reflect post-bloom production. Indeed, an early bloom was reported in May 2008 in the Amundsen Gulf, East of the Beaufort Sea (Brown et al., 2011; Belt et al., 2013) although this does not imply that the Northwind Ridge experienced similar production growth. By contrast, a deep sediment trap in the southwestern Canadian Basin indicates high POC values in August and September 2008, which based on a sinking velocity of 85 m d^{-1}, corresponds to high surface production and export in July - August (Station A in Fig. 1; Hwang et al., 2015; Onodera et al., 2015). Furthermore, ice-ocean-ecosystem coupled model simulations point out peaking chlorophyll-*a* values in the Chukchi Sea in August 2008 (Wang et al., 2013). Therefore, we can reasonably infer that the diatom flux measured in August 2008 represents the blooming season locally and that it was thus lower than in 2009. This assumption is further supported by MODIS summer sea surface chlorophyll-*a* concentrations of the area indicating ~36% higher values in 2009 (0.382 µg l^{-1}) than 2008 (0.282 µg l^{-1}).

Biogenic production at DM is influenced by the PWI, the oligotrophic waters of the BG and the sea ice distribution during the blooming season (Fig. 1). The Arctic Oscillation (AO) plays an important role on sea ice distribution and surface ocean circulation (Rigor et al., 2002; Serreze et al., 2003; Steele et al., 2004).

Since 1997, the BG circulation is driven by an anticyclonic wind circulation resulting in enhanced freshening of the BG waters (Giles et al., 2012; Rabe et al., 2014; Proshutinsky et al., 2015; Wang et al., 2018). The subsequent stratification prevents nutrient to replenish the upper

ocean and thus stalls phytoplankton growth (McLaughlin and Carmack, 2010). The strength of the BG is linked to the Arctic Ocean Oscillation (AOO) index, which varied annually and notably shifted from a strong BG (AOO index = 2.9) in 2008 to a weaker BG in 2009 (AOO index = 1.9; Fig. 4a) (Proshutinsky et al., 1999, 2015). We can thus hypothesize that phytoplankton productivity at DM in 2008 was limited by stratified conditions maintaining oligotrophic conditions in the upper ocean due to freshening under intensified BG. Likewise, weakened and reduced BG in 2009 provided more favorable conditions for refueling surface waters in nutrients to sustain higher production. This is consistent with fresher surface waters reported near DM in summer 2008 than summer 2009 (Zhang, 2009; Kikuchi, 2009). Model results also show prevailing west-northwestward surface flow in the Chukchi Borderland in summer 2008 carrying nutrient-depleted waters from the Beaufort Sea to DM, whereas in summer 2009 the surface ocean circulation was nearly northward bringing nutrient-rich PWI waters to our site (Onodera et al., 2015). These findings highlight the key role of atmospheric conditions in driving the surface current and nutrients transport at the BG boundary and their impact on diatom flux.

The PWI is regarded as a pivotal nutrient source for the Arctic Ocean ecosystem (Walsh et al., 1997). The mean annual transport of the PWI through the Bering Strait (~0.8 Sv) fluctuates seasonally as well as annually (Roach et al., 1995; Woodgate et al., 2015) around values that regularly increased since 1990 (Woodgate et al., 2012; Woodgate, 2018). The PWI in summer 2009 (~1.7 Sv) was stronger than in 2008 (~1.35 Sv) (Fig. 4b). Furthermore, during its maximum transport period (April to July) this flow was ~0.2 Sv higher in 2009 than 2008. Based on the distance between the Bering Strait and DM and current velocities in the Chukchi Sea (Weingartner et al., 2005; Woodgate et al., 2005b), we can estimate that ~4 months is needed for the PWI to reach our mooring site, which is in agreement with the time lag between the PWI peak and high biogenic production in summer 2009 (Fig. 4). It is thus very reasonable to conclude that stronger PWI by entraining more nutrients into the Arctic Ocean likely triggered enhanced phytoplankton production in 2009.

The sea ice distribution during summer also shows different patterns in 2008 and 2009 (Fig. 5). As expected from AO and subsequent ocean circulation, in 2008 sea ice started retreating westwards from the East, favoring the inflow of freshened and oligotrophic BG waters. Meanwhile, the presence of sea ice in the South likely prevented nutrient-rich PWI waters from advecting to our site. In contrast, sea ice melting in 2009 began from the South allowing the PWI to flow to DM and influence primary production. This is further supported by surface wind fields shown in Fig. S1. Easterly winds in July 2008 favored transport of freshened and oligotrophic waters from the BG towards to the northwest or North of DM thereby limiting biogenic production. In August 2008, southward winds further contributed to counteract the

northward advection of PWI, whereas in summer 2009 (July and August) Northerly winds enhanced transport of nutrient-rich PWI to our mooring site, favoring diatom blooming (Fig. S1)

In summary, our results provide consistent evidences on the impact of contrasting atmospheric and oceanic circulation, notably the BG circulation, PWI nutrient transport as well as sea ice retreat pattern on diatoms fluxes in the Chukchi Sea, between 2008 and 2009 (Fig. 5). They also underline that the southern Northwind Ridge is an area of strong interactions between water masses from the Canadian Basin, the Pacific and even coastal Siberia, where seasonal sea ice drift and motion makes it a sensitive region to ongoing climate change.

5.2 Lateral transport of diatoms

Coastal diatoms, mostly dwelling in the continental shelf area, are indicative of lateral advection from the nearby Chukchi Sea shelf waters. Previous studies have shown that while *Paralia sulcata* prevails in the sediments of the Chukchi Sea Shelf, this species is rarely found in the Chukchi Borderland (Ran et al., 2013). At DM, the coastal diatom fluxes are also dominated by *P. sulcata* peaking in September 2009, pointing out a significant influence of water masses from the shelf area under stronger PWI conditions (Fig. 6b; See 5.1; Woodgate, 2018). Apart from this episode, values were low and stable (Fig. 6b).

Chaetoceros RS is also considered as an indicator of allochthonous material (Onodera et al., 2015). In our dataset *Chaetoceros* RS displays similar seasonal pattern as terrigenous biomarker campesterol and β-sitosterol (Fig. 6c-d). The flux of these biomarkers produced by higher plants (Huang and Meinschein, 1976) were found to also parallel lithogenic matter fluxes in both shallow and deep sediment traps of the central Arctic Ocean (Fahl and Nöthig, 2007). The co-eval temporal evolution of terrigenous sterols and lithogenic material at DM is consistent with lateral advection from the shelf in summer of 2009 (Fig. 6d-e). In contrast, the lithogenic matter content (in %) drops to its lowest values in summer 2009 witnessing a reduced contribution of allochthonous material (Fig. 6b-d, f). This discrepancy cannot be explained by sea ice transport of coastal diatoms and biomarkers in winter and later settling under ice-free conditions in September 2009 (Fig. 6a). Besides, this mechanism cannot account either for the concomitant decrease of lithogenic matter content in summer 2009. Another explanation is that coastal diatoms and terrigenous material might be entrained by PWI. Enhanced PWI would thus be responsible for higher phytoplankton production in summer 2009 and the advection of terrigenous matter (See 5.1). This is further supported by the decrease of the C/N ratio (bulk organic carbon over bulk organic nitrogen mole ratio; modified from Bai et al, 2019) to 6.4 in summer 2009. This value, close to the Redfield ratio of 6.6, points out a major marine origin of settling material (Fig. 6g). Boosted blooming production and export of organic matter likely

explain enhanced contribution of marine constituents to the overall flux and the subsequent decline of lithogenic content (Fig. 6f).

The abundance and flux of lithogenic matter, mostly composed of silt and clay, are higher at our site than at nearby mooring station NAP and LOMO2 (Fig. 1) in the central Arctic, despite a difference in water depths. Lithogenic particles might be derived from a proximate branch of the Northwind Ridge, lying at ~900 m water depth (Poore et al., 1994), close to the depth of our sediment trap (~870 m). Benthic nepheloid layer developing hundreds meters above the seafloor is another possible mechanism able to remobilize sediments from the Northwind Ridge and transport them to the sediment trap location (Rutgers van der Loeff et al., 2002).

5.3 Sea ice diatoms and IP_{25}

Fluxes of sea ice diatoms and IP_{25} at DM display quite similar seasonal patterns (Fig. 7a). Since IP_{25} is produced by specific sea ice diatoms (Brown et al., 2014), some correlation is expected between the two fluxes ($n = 21$; $r^2 = 0.64$; $p < 0.01$; Fig. 7b; Table 2). This correlation is statistically unchanged after discarding low flux values ($IP_{25} < 0.5$ ng $m^{-2}d^{-1}$; sea ice diatom $< 1 \times 10^5$ valves m^{-2} d^{-1}) ($n = 13$; $r^2 = 0.61$; $p < 0.01$). Both fluxes are high during the sea ice melting season for both years. Although sea ice reconstructions based on micropaleontological fossils or biomarkers preserved in the sediment cores have been successfully carried out in the Atlantic and Arctic Ocean (e.g. diatoms: Sha et al., 2016, 2017; IP_{25}: Massé et al., 2008; Müller et al., 2009; Vare et al., 2009; Müller and Stein, 2014; Belt et al., 2015; Xiao et al., 2015; Cabedo-Sanz et al., 2016; Hörner et al., 2016, 2017; Stein et al., 2016, 2017; Kolling et al., 2017; Clotten et al., 2018; Kremer et al., 2018), they have rarely been produced and compared in the same core. Few available studies show poor agreement between sea ice diatoms and IP_{25}, a result that might be attributed to the specificity of IP_{25} producers as opposed to the broader habitat of sea ice diatoms (Weckström et al., 2013; Sha et al., 2015). Our sediment trap record, however, indicates consistent and synchronous fluctuations of the sea ice diatom group and IP_{25} fluxes with respect to sea ice distribution (Fig. 7a). Departures of diatom versus biomarker signals in sediments can, to some extent, be attributed to dissolution and degradation (Belt and Müller, 2013). Previous studies in the Arctic have shown that IP_{25} is biosynthesized by sea ice diatoms *Haslea crucigeroides* and *Pleurosigma stuxbergii* var. *rhomboides* (Belt et al., 2013; Brown et al., 2014). These species are present in our sediment trap in summer mainly during high IP_{25} fluxes (Fig. 7a). Although these species have been frequently reported at the bottom sea ice and, to a lesser extent, in the water column in the Arctic (e.g. von Quillfeldt, 1997; von Quillfeldt et al., 2003; Katsuki et al., 2009), they were identified in only a few summer samples at ~870 m, possibly because of dissolution during settling. These species have seldomly been found in Arctic sediments (e.g. Ran et al., 2013; Obrezkova et al., 2014; Astakhov et al., 2015;

Limoges et al., 2018). The non-IP_{25} producing sea ice diatoms, e.g. *Fossula arctica*, *Fragilariopsis cylindrus*, *F. oceanica*, also suffer from dissolution. Sediment trap data from the Nordic Seas have shown that weakly silicified diatoms strongly dissolve in the sediments while the robust ones are preserved (Kohly, 1998). Selective degradation of diatom frustules was also demonstrated by comparing diatoms from shallow and deep traps at the nearby mooring site NAP (Onodera et al., 2015). The relative abundance of *Rhizosolenia* spp., for instance, decreased remarkably in the deep trap, whereas some diatom taxa increased in the abyssal material (Onodera et al., 2015). In another study in the Chukchi Sea, the diatom assemblages in sea ice and underlying sediments showed significant differences (von Quillfeldt et al., 2003). Despite the fact that the diatom composition and species diversity of sediment trap at DM are comparable to those of the sediments in the northern Chukchi Sea, weakly silicified diatoms, *Chaetoceros* RS and sea ice diatoms among others, became less abundant in the sediments while diatoms with stronger frustules such as *Thalassiosira antarctica* var. *borealis* RS increased (Table 1; Ran et al., 2013). This finding supports the idea of selective diatom dissolution during export to deep sediments, which pleas for cautious interpretation of paleo-reconstructions. In contrast, given its low photo-reactivity and wide distribution in the Arctic sediments, IP_{25} should introduce less bias due to diagenesis (Brown and Belt, 2012; Belt and Müller, 2013). Although a possible biogeochemical degradation of IP_{25} was suggested in the central Arctic based on shallow and deep sediment traps, the IP_{25} seasonal patterns remained similar from 150 to 1550 m water depth (Fahl and Stein, 2012). Nevertheless, investigations are needed to explore IP_{25} degradation and its possible impact on past sea ice reconstruction.

Major phytosterols, namely brassicasterol and dinosterol, show a high correlation with cold-water diatoms ($r^2 = 0.83$ and 0.77, respectively; $p < 0.01$; Table 2). From this result we can infer that both phytosterol producers and cold-water diatoms thrive in ice-free conditions (Bai et al., 2019). Cold-water diatoms, however, have been also reported underneath consolidated sea ice (Arrigo et al, 2012, 2014). In this case, it is expected that both cold-water and sea ice diatoms sink synchronously and result in a significant correlation between their respective fluxes ($r^2 = 0.64$; $p < 0.01$; Table 2). Interestingly, the tri-unsaturated highly branched isoprenoid alkene (HBI-III), presumably associated with marginal ice zone (Belt et al., 2015; Smik et al., 2016; Smik and Belt, 2017; Bai et al., 2019), shows a weak correlation with the sea ice diatom flux ($r^2 = 0.48$; $p < 0.01$; Table 2). Although HBI-III producers have not yet been fully recognized, the hypothesized producers are within diatom genera *Pleurosigma* and *Rhizosolenia* (Belt, 2018; Belt et al., 2000, 2015; Rowland et al., 2001). In this area diatom species belonging to *Pleurosigma* are mainly related to sea ice while *Rhizosolenia* is found in the ice-free waters (von Quillfeldt et al., 2003; Onodera et al., 2015). The weak correlation between HBI-III and sea ice diatoms rather hints a sea ice source or sea ice edge conditions, but more investigation

is needed to be more conclusive.

Diatom sinking velocity of >85 m d^{-1} in summer has been recently estimated based on the time lag between the shallow and deep trap diatom fluxes at NAP (Onodera et al., 2015). Using this value, the summer diatom flux at ~870 m water depth at our site should represent the export of material from surface waters or the sea ice produced about 10 days earlier. Hence, the diatom bloom of summer 2009 might have started early July when the sea ice was about to retreat but still compact (Fig. 2, 5). Incidentally, massive under sea ice phytoplankton blooms have been observed in the Beaufort Sea in summer 2008 (Mundy et al., 2009) and in the Chukchi Sea in summer 2011, maximizing at >100 km into the sea ice cover boundary (Arrigo et al., 2012, 2014). This phenomenon was attributable to intensified light penetration through sea ice into the water column due to more melt ponds (Arrigo et al., 2014; Mundy et al., 2014). Thawing snow over sea ice as well as leads in the ice pack might also have played a role in promoting under ice bloom (Ambrose et al., 2005; Różańska et al., 2009; Arrigo, 2017; Assmy et al., 2017; Lalande et al., 2019). Although no melt ponds data exist at DM for summer 2009, on-site model estimates indicate that the snow cover had almost vanished and the sea ice thickness decreased from ~2.8 m to ~1.5 m, at that time of maximum solar irradiance (Fig. 2a-d), leading to similar sea surface state in summer 2009 as in 2011, allowing light penetration to trigger under sea ice bloom.

6. Conclusions

The one-year long sediment trap time-series (August 2008 - September 2009, ~870 m water depths) from the southern Northwind Ridge in the western Arctic Ocean highlights the strong seasonality of diatom abundances and fluxes. *Chaetoceros* RS and, to a lesser extent, the sea ice diatoms, e.g. *Fossula arctica*, *Fragilariopsis cylindrus*, *F. oceanica*, dominate the diatom composition.

Diatom fluxes are two- to three-fold higher in summer 2009 than in summer 2008, a result that is explained by a weaker BG circulation, an intensified PWI bringing nutrients into the Arctic Ocean and the earlier retreat of sea ice from the South in 2009. Our findings underline the sensitivity of the southern Northwind Ridge export fluxes to the spatio-temporal pattern of sea ice melting and upper ocean circulation regime.

High fluxes of coastal diatoms, terrigenous biomarkers and lithogenic matter show indicate lateral advection in summer 2009 likely triggered by enhanced PWI rather than by drifting sea ice.

Sea ice diatom fluxes are coherent with IP_{25} fluxes, both showing high values during the sea ice melting period reflecting marginal ice zone conditions. However, sea ice diatoms might be prone to selective dissolution in the water column that is likely to alter diatom assemblage

in sediments and introduce bias in sea ice reconstructions. This result reinforces the need for multi-proxy approaches to assess proxy biases and improve past sea ice estimates.

Acknowledgements

We are grateful to the captain, crew members and scientific party of the R/V *Xuelong* for deployment and recovery of the sediment trap. We are deeply indebted to Dr. M.S. Obrezkova of V.I. Ilyichev Pacific Oceanological Institute, Russian Academy of Sciences, for her kind help on diatom taxonomy. Dr. Leonid Polyak of Ohio State University is acknowledged for his helpful advices. We also thank Dr. Zhengbing Han and Dr. Qingsheng Guan of Second Institute of Oceanography for technical assistance. This study was funded by the Scientific Research Funds of the Second Institute of Oceanography, State Oceanic Administration, China (Nos. JG1611, JG1911), the National Natural Science Foundation of China (Nos. 41606052, 41976229, 41806228, 41306200), the Chinese Polar Environmental Comprehensive Investigation and Assessment Programs (No. CHINARE 0304), National Postdoctoral Foundation of China (No. 17090093) and the Cai Yuanpei Program/ICAR (Sea Ice melt, Carbon, Acidification and Phytoplankton in the present and past Arctic Ocean) funded by China Scholarship Council. We thank the Centre National de la Recherche Scientifique (CNRS) for M.-A.S. salary. We also thank three anonymous reviewers for valuable comments to improve the manuscript.

Author contributions

J. R. designed the study and wrote the manuscript with contribution of M.-A. S., J. C., H. L., J. Z., Y. B., Y. Z and B. W. J. R. carried out the diatom identification. Y. B. and Y. L. contributed the biomarker analyses (campesterol and β-sitosterol), J. Z. performed the determination of particulate inorganic carbon (PIC) and calculated the CaCO3 content. Z. J. and H. J. contributed the particulate organic carbon (POC) and B. W. the opal flux. Z. Y. and L. L. retrieved the environmental data from different database. All authors contributed to the final version of the manuscript.

Declarations of interest: None

References

Abelmann, A., 1992. Diatom assemblages in Arctic sea ice: indicator for ice drift pathways. Deep-Sea Research, 39, 525-538.

Ambrose, W.G. Jr, von Quillfeldt, C., Clough, L.M., Tilney, P.V.R., Tucker, T., 2005. The sub-ice algal community in the Chukchi Sea: large- and small-scale patterns of abundance based on images from a remotely operated vehicle. Polar Biology, 28, 784–795.

Arrigo, K.R., 2017. Sea ice as a habitat for primary producers. In: Thomas, D.N. (Ed.), Sea Ice, 3rd ed. John Wiley & Sons, Chichester, pp. 352–369.

Arrigo, K.R., van Dijken, G.L., 2015. Continued increases in Arctic Ocean primary production. Progress in Oceanography, 136, 60-70.

Arrigo, K.R., Dijken, G.V., Pabi, S., 2008. Impact of a shrinking Arctic ice cover on marine primary production. Geophysical Research Letters 35, L19603. https://doi.org/10.1029/2008GL035028.

Arrigo, K.R., Perovich, D.K., Pickart, R.S., Brown, Z.W., van Dijken, G.L., Lowry, K.E., Mills, M.M., Palmer, M.A., Balch, W.M., Bahr, F., Bates, N.R., Benitez-Nelson, C., Bowler, B., Brownlee, E., Ehn, J.K., Frey, K.E., Garley, R., Laney, S.R., Lubelczyk, L., Mathis, J., Matsuoka, A., Mitchell, B.G., Moore, G.W.K., Ortega-Retuerta, E., Pal, S., Polashenski, C.M., Reynolds, R.A., Schieber, B., Sosik, H.M., Stephens, M., Swift, J.H., 2012. Massive phytoplankton blooms under Arctic sea ice. Science, 336, 1408 – 1408.

Arrigo, K.R., Perovich, D.K., Pickart, R.S., Brown, Z.W., van Dijken, G.L., Lowry, K.E., Mills, M.M., Palmer, M.A., Balch, W.M., Bates, N.R., Benitez-Nelson, C.R., Brownlee, E., Frey, K.E., Laney, S.R., Mathis, J., Matsuoka, A., Greg Mitchell, B., Moore, G.W.K., Reynolds, R.A., Sosik, H.M., Swift, J.H., 2014. Phytoplankton blooms beneath the sea ice in the Chukchi Sea. Deep-Sea Research Part II, 105, 1–16.

Ardyna, M., Babin, M., Gosselin, M., Devred, E., Rainville, L., Tremblay, J.-É., 2014. Recent Arctic Ocean sea ice loss triggers novel fall phytoplankton blooms. Geophysical Research Letters, 41, doi:10.1002/2014GL061047.

Assmy, P., Fernandezmendez, M., Duarte, P., Meyer, A., Randelhoff, A., Mundy, C. J., et al., 2017. Leads in Arctic pack ice enable early phytoplankton blooms below snow-covered sea ice. Scientific Reports, 7, 40850.

Astakhov, A.S., Bosin, A.A., Kolesnik, A.N., Obrezkova, M.S., 2015. Sediment geochemistry and diatom distribution in the Chukchi Sea: Application for bioproductivity and paleoceanography. Oceanography, 28, 190–201.

Bai, Y., Sicre, M.-A., Chen, J., Klein, V., Jin, H., Ren, J., Li, H., Xue, B., Ji, Z., Zhuang, Y., Zhao, M., 2019. Seasonal and spatial variability of sea ice and phytoplankton biomarker flux in the Chukchi Sea (western Arctic Ocean). Progress in Oceanography, 171, 22–37.

Belt, S.T., 2018. Source-specific biomarkers as proxies for Arctic and Antarctic sea ice. Organic Geochemistry, 125, 277-298.

Belt, S.T., 2019. What do IP_{25} and related biomarkers really reveal about sea ice change? Quaternary Science Reviews, 204, 216-219.

Belt, S.T., Allard, W.G., Massé, G., Robert, J.-M., Rowland, S.J., 2000. Highly branched isoprenoids (HBIs): identification of the most common and abundant sedimentary isomers. Geochimica et Cosmochimica Acta, 64, 3839–3851.

Belt, S.T., Müller, J., 2013. The Arctic sea ice biomarker IP_{25}: a review of current understanding, recommendations for future research and applications in palaeo sea ice reconstructions. Quaternary Science Review, 79, 9–25.

Belt, S.T., Brown, T.A., Ringrose, A.E., Cabedo-Sanz, P., Mundy, C.J., Gosselin, M., Poulin, M., 2013. Quantitative measurement of the sea ice diatom biomarker IP_{25} and sterols in Arctic sea ice and underlying sediments: Further considerations for palaeo sea ice reconstruction. Organic Geochemistry, 62, 33–45.

Belt, S.T., Cabedo-Sanz, P., Smik, L., Navarro-Rodriguez, A., Berben, S.M.P., Knies, J., Husum, K., 2015. Identification of paleo Arctic winter sea ice limits and the marginal ice zone: Optimised biomarker-based reconstructions of late Quaternary Arctic sea ice. Earth and Planetary Science Letter, 431, 127–139.

Bluhm, B.A., Gebruk, A.V., Gradinger, R., Hopcroft, R.R., Huettmann, F., Kosobokova, K.N.,

630 Sirenko, B.I., Weslawski, J.M., 2011. Arctic marine biodiversity: An update of species richness
631 and examples of biodiversity change. Oceanography, 24, 232–248.
632
633 Boetius, A., Albrecht, S., Bakker, K., Bienhold, C., Felden, J., Fernandez-Mendez, M.,
634 Hendricks, S., Katlein, C., Lalande, C., Krumpen, T., Nicolaus, M., Peeken, I., Rabe, B.,
635 Rogacheva, A., Rybakova, E., Somavilla, R., Wenzhofer, F., 2013. Export of algal biomass from
636 the melting Arctic sea ice. Science, 339, 1430–1432.
637
638 Booth, B.C. and Horner, R.A., 1997. Microalgae on the Arctic Ocean section, 1994: species
639 abundance and biomass. Deep-Sea Research, 2, 44, 1607–1622.
640
641 Brown, T.A., Belt, S.T., 2012. Identification of the sea ice diatom biomarker IP25 in Arctic
642 benthic macrofauna: direct evidence for a sea ice diatom diet in Arctic heterotrophs. Polar
643 Biology, 35, 131-137.
644
645 Brown, T.A., Belt, S.T., Mundy, C., Philippe, B., Massé, G., Poulin, M., Gosselin, M., 2011.
646 Temporal and vertical variations of lipid biomarkers during a bottom ice diatom bloom in the
647 Canadian Beaufort Sea: further evidence for the use of the IP25 biomarker as a proxy for spring
648 Arctic sea ice. Polar Biology, 34, 1857–1868.
649
650 Brown, T.A., Belt, S.T., Tatarek, A., Mundy, C.J., 2014. Source identification of the Arctic sea
651 ice proxy IP25. Nature Communications, 5, 4197.
652
653 Cabedosanz, P., Belt, S. T., Jennings, A. E., Andrews, J. T., & Geirsdottir, A., 2016). Variability
654 in drift ice export from the Arctic Ocean to the North Icelandic Shelf over the last 8000 years:
655 A multi-proxy evaluation. Quaternary Science Reviews, 146, 99-115.
656
657 Carroll, M.L., Carroll, J., 2003. The Arctic Seas. In: Black, K., Shimmield, G. (Eds.),
658 Biogeochemistry of Marine Systems. Blackwell Publishing, Oxford, pp. 127–156.
659
660 Cavalieri, D.J., Parkinson, C.L., Gloersen, P., Zwally, H.J., 1996, updated yearly. Sea Ice
661 Concentrations from Nimbus-7 SMMR and DMSP SSM/I-SSMIS Passive Microwave Data,
662 Version 1. [Indicate subset used]. Boulder, Colorado USA. NASA National Snow and Ice Data
663 Center Distributed Active Archive Center. doi: https://doi.org/10.5067/8GQ8LZQVL0VL.
664
665 Clotten, C., Stein, R., Fahl, K., De Schepper, S., 2018. Seasonal sea ice cover during the warm
666 Pliocene: Evidence from the Iceland Sea (ODP Site 907). Earth and Planetary Science Letters,

481, 61-72.

Coachman, L.K., Aagaard, K., 1966. On the water exchange through Bering Strait. Limnology and Oceanography, 11, 44-59.

Comiso, J.C., 2012. Large decadal decline of the Arctic multiyear ice cover. Journal of Climate, 25, 1176–1193.

Coupel, P., Jin, H., Joo, M., Horner, R., Bouvet, H.A., Sicre, M.-A., Gascard, J.-C., Chen, J.F., Garçon, V., Ruiz-Pino, D., 2012. Phytoplankton distribution in unusually low sea ice cover over the Pacific Arctic. Biogeosciences 9, 4835–4850.

Coupel, P., Ruiz-Pino, D., Sicre, M.A., Chen, J., Lee, S., Schiffrine, N., Li, H., Gascard, J.C., 2015. The impact of freshening on phytoplankton production in the Pacific Arctic Ocean. Progress in Oceanography, 131, 113–125.

Esper, O., Gersonde, R., Kadagies, N., 2010. Diatom distribution in southeastern Pacific surface sediments and their relationship to modern environmental variables. Palaeogeography, Palaeoclimatology, Palaeoecology, 287, 1-27.

Fahl, K., Stein, R., 2012. Modern seasonal variability and deglacial/Holocene change of central Arctic Ocean sea-ice cover: New insights from biomarker proxy records. Earth and Planetary Science Letters, 351–352, 123–133.

Fahl, K., Nöthig, E.M., 2007. Lithogenic and biogenic particle fluxes on the Lomonosov Ridge (central Arctic Ocean) and their relevance for sediment accumulation: Vertical vs. lateral transport. Deep-Sea Research Part I, 54, 1256–1272.

Fleming, W.D., 1954. Naphrax: a synthetic mounting medium of high refractive index new and improved methods of preparation. Journal of Microscopy, https://doi.org/10.1111/j.1365-2818.1954.tb02001.x.

Forest, A., Sampei, M., Hattori, H., Makabe, R., Sasaki, H., Fukuchi, M., Wassmann, P., and Fortier, L., 2007. Particulate organic carbon fluxes on the slope of the Mackenzie Shelf (Beaufort Sea): Physical and biological forcing of shelf-basin exchanges. Journal of Marine Systems, 68, 39–54.

Forest, A., Sampei, M., Makabe, R., Sasaki, H., Barber, D., Gratton, Y., Wassmann, P., Fortier, L., 2008. The annual cycle of particulate organic carbon export in Franklin Bay (Canadian Arctic): environmental control and food web implications. Journal of Geophysical Research: Oceans 113, C03S05. doi:10.1029/2007JC004262.

Forest, A., Tremblay, J.-E., Gratton, Y., Martin, J., Gagnon, J., Darnis, G., Sampei, M., Fortier, L., Ardyna, M., Gosselin, M., Hattori, H., Nguyen, D., Maranger, R., Vaqué, D., Pedrós-Alió, C., Sallon, A., Michel, C., Kellogg, C., Deming, J., Shadwick, E., Thomas, H., Link, H., Archambault, P., Piepenburg, D., 2011. Biogenic carbon flows through the planktonic food web of the Amundsen Gulf (Arctic Ocean): a synthesis of field measurements and inverse modeling analyses. Progress in Oceanography, 91, 410–436.

Gersonde, R., Zielinski, U., 2000. The reconstruction of late Quaternary Antarctic sea ice distribution — the use of diatoms as a proxy for sea ice. Palaeogeography, Palaeoclimatology, Palaeoecology, 162, 263–286.

Giles, K.A., Laxon, S.W., Ridout, A.L., Wingham, D.J., Bacon, S., 2012. Western Arctic Ocean freshwater storage increased by wind-drivenspin-up of the Beaufort Gyre. Nature Geoscience, 5, 194–197.

Grebmeier, G.M., 2012. Shifting patterns of life in the Pacifi c Arctic and sub-Arctic Seas. Annual Review of Marine Science, 4, 16.1–16.16.

Grebmeier, J.M., Cooper, L.W., Feder, H.M., Sirenko, B.I., 2006. Ecosystem dynamics of the Pacific-influenced northern Bering and Chukchi seas in the Amerasian Arctic. Progress in Oceanography, 71, 331–361.

Harada, N., 2016. Review: Potential catastrophic reduction of sea ice in the western Arctic Ocean: Its impact on biogeochemical cycles and marine ecosystems. Global and Planetary Change, 136, 1–17.

Hasle, G.R., Syvertsen, E.E., 1997. Marine diatoms. In: Tomas, C.R. (Ed.), Identifying Marine Phytoplankton. Academic Press, New York, pp. 5–385.

He, J., Zhang, F., Lin, L., Ma, Y., Chen, J., 2012. Bacterioplankton and picophytoplankton abundance, biomass, and distribution in the Western Canada Basin during summer 2008. Deep-

741 Sea Research Part II, 81–84, 36–45.
742
743 Honjo, S., Krishfield, R. A., Eglinton, T. I., Manganini, S. J., Kemp, J. N., Doherty, K., Hwang,
744 J., McKee, T. K., and Takizawa, T., 2010. Biological pump processes in the cryopelagic and
745 hemipelagic Arctic Ocean: Canada Basin and Chukchi Rise. Progress in Oceanography, 85,
746 137–170.
747
748 Hörner ,T., Stein, R., Fahl, K., Birgel, D., 2016. Post-glacial variability of sea ice cover, river
749 run-off and biological production in the western Laptev Sea (Arctic Ocean) – a high-resolution
750 biomarker study. Quaternary Science Review, 143, 133–149.
751
752 Hörner, T., Stein, R., Fahl, K., 2017. Evidence for Holocene centennial variability in sea ice
753 cover based on IP25 biomarker reconstruction in the southern Kara Sea (Arctic Ocean). Geo-
754 marine Letters, 37, 515-526.
755
756 Huang, W.Y., Meinschein, W.G., 1976. Sterols as source indicators of organic material in
757 sediments. Geochimica et Cosmochimica Acta, 40, 323–330.
758
759 Hwang, J., Kim, M., Manganini, S. J., Mcintyre, C., Haghipour, N., Park, J., Krishfield, R.A.,
760 Macdonald, R.W., Eglinton, T. I., 2015. Temporal and spatial variability of particle transport in
761 the deep Arctic Canada Basin. Journal of Geophysical Research: Oceans, 120, 2784-2799.
762
763 Ikenoue, T., Bjørklund, K.R., Krugulikova, S.B., Onodera, J., Kimoto, K., Harada, N., 2015.
764 Flux variations and vertical distributions of siliceous Rhizaria (Radiolaria and Phaeodaria) in
765 the western Arctic Ocean: indices of environmental changes. Biogeosciences, 12, 2019–2046.
766
767 Joo, H.M., Lee, S.H., Jung, S.W., Dahms, H.-U., Lee, J.H., 2012. Latitudinal variation of
768 phytoplankton communities in the western Arctic Ocean. Deep-Sea Research Part II, 81–84, 3–
769 17, 2012.
770
771 Jousé, A.P., Kozlova, O.G., Muhina, V.V., 1971. Distribution of diatoms in the surface layer of
772 sediment from the Pacific Ocean. In: Funnell, B.M., Riedel, W.R. (Eds.), The
773 Micropalaeontology of Oceans. Cambridge University Press, London, pp. 263–269.
774
775 Katsuki, K., Takahashi, K., Onodera, J., Jordan, R.W., Suto, I., 2009. Living diatoms in the
776 vicinity of the North Pole, summer 2004. Micropaleontology, 55, 137-170.
777

Kikuchi, T., 2009. R/V *Mirai* Cruise Report MR09–03. JAMSTEC, Yokosuka, 190p.

Kohly, A., 1998. Diatom flux and species composition in the Greenland Sea and the Norwegian Sea in 1991–1992. Marine Geology, 145, 293-312.

Kolling, H.M., Stein, R., Fahl, K., Perner, K., Moros, M., 2017. Shortterm variability in late Holocene sea ice cover on the East Greenland Shelf and its driving mechanisms. Palaeogeography, Palaeoclimatology, Palaeoecology, 485, 336–350.

Kremer, A., Stein, R., Fahl, K., Ji, Z., Yang, Z., Wiers, S., Matthiessen, J., Forwick, M., Löwemark, L., O'Regan, M., Chen, J., Snowball, I., 2018. Changes in sea ice cover and ice sheet extent at the Yermak Plateau during the last 160 ka—reconstructions from biomarker records. Quaternary Science Reviews, 182, 93-108.

Lalande, C., Bélanger, S., Fortier, L., 2009. Impact of a decreasing sea ice cover on the vertical export of particulate organic carbon in the northern Laptev Sea, Siberian Arctic Ocean. Geophysical Research Letters, 36, L21604, doi:10.1029/2009GL040570.

Lalande, C., Nöthig, E.-M., Somavilla, R., Bauerfeind, E., Shevchenko, V., Kolodkov, Y., 2014. Variability in under-ice export fluxes of biogenic matter in the Arctic Ocean. Global Biogeochemical Cycle, 28, 571–583, doi:10.1002/2013GB004735.

Lalande, C., Nöthig, E.-M., Fortier, L., 2019. Algal export in the Arctic Ocean in times of global warming. Geophysical Research Letters, 46, https://doi.org/10.1029/2019GL083167.

Lee, Y., Min, J.-O., Yang, E.J., Cho, K.-H., Jung, J., Park, J., Moon, J.K., Kang, S.-H., 2019. Influence of sea ice concentration on phytoplankton community structure in the Chukchi and East Siberian Seas, Pacific Arctic Ocean. Deep-Sea Research Part I, doi: https://doi.org/10.1016/j.dsr.2019.04.001.

Li, W.K., Mclaughlin, F.A., Lovejoy, C., Carmack, E.C., 2009. Smallest algae thrive as the Arctic Ocean freshens. Science, 326, 539.

Limoges, A., Massé, G., Weckström, K., Poulin, M., Ellegaard, M., Heikkila, M., Geilfus, N.-X., Sejr, M.K., Rysgaard, S., Ribeiro, S., 2018. Spring succession and vertical export of diatoms and IP25 in a seasonally ice-covered high arctic fjord. Frontiers of Earth Science, 6, 226, doi: 10.3389/feart.2018.00226.

Mantua, N.J., Hare, S.R., Zhang, Y., Wallace, J.M., Francis, R.C., 1997. A Pacific interdecadal climate oscillation with impacts on salmon production. Bulletin of the American Meteorological Society, 78, pp. 1069-1079.

Matsuno, K., Yamaguchi, A., Fujiwara, A., Onodera, J., Watanabe, E., Imai, I., Chiba, S., Harada, N., Kikuchi, T., 2014. Seasonal changes in mesozooplankton swimmers collected by sediment trap moored at a single station on the Northwind Abyssal Plain in the western Arctic Ocean. Journal of Plankton Research, 36, 490–502.

McLaughlin, F.A., Carmack, E., 2010. Deepening of the nutricline and chlorophyll maximum in the Canada Basin interior, 2003–2009. Geophysical Research Letters, 37, L24602. http://dx.doi.org/10.1029/2010GL045459.

McLaughlin, F., Carmack, E., Proshutinsky, A., Krishfield, R.A., Guay, C., Yamamoto-Kawai, M., Jackson, J.M., Williams, B., 2011. The rapid response of the Canada Basin to climate forcing: From bellwether to alarm bells. Oceanography, 24, 146–159.

Medlin, L.K., Priddle, J., 1990. Polar Marine Diatoms. British Antarctic Survey, Cambridge, 214 pp.

Miettinen, A., 2018. Diatoms in Arctic regions: Potential tools to decipher environmental changes. Polar Science, 18, 220-226.

Miettinen, A., Koc, N., Husum, K., 2013. Appearance of the Pacific diatom Neodenticula seminae in the northern Nordic Seas — an indication of changes in Arctic sea ice and ocean circulation. Marine Micropaleontology, 99, 2-7.

Mundy, C.J., Gosselin, M., Ehn, J., Gratton, Y., Rossnagel, A., Barber, D.G., Martin, J., Tremblay, J.-E., Palmer, M., Arrigo, K.R., Darnis, G., Fortier, L., Else, B., Papakyriakou, T., 2009. Contribution of under-ice primary production to an ice-edge upwelling phytoplankton bloom in the Canadian Beaufort Sea. Geophysical Research Letters, 36, L17601.

Mundy, C.J., Gosselin, M., Gratton, Y., Brown, K.A., Galindo, V., Campbell, K., Levasseur, M., Barber, D., Papakyriakou, T., Belanger, S., 2014. Role of environmental factors on phytoplankton bloom initiation under landfast sea ice in Resolute Passage, Canada. Marine

852 Ecology Progress Series, 497, 39-49.
853
854 Müller, P. J., Suess, E. Andréungerer, C., 1986. Amino acids and amino sugars of surface
855 particulate and sediment trap material from waters of the Scotia Sea. Deep-Sea Research Part
856 I, 33, 819–838.
857
858 Müller, J., Stein, R., 2014. High-resolution record of late glacial and deglacial sea ice changes
859 in Fram Strait corroborates ice–ocean interactions during abrupt climate shifts. Earth and
860 Planetary Science Letter, 403, 446–455.
861
862 Müller, J., Massé, G., Stein, R., Belt, S.T., 2009. Variability of sea-ice conditions in the Fram
863 Strait over the past 30,000 years. Nature Geoscience, 2, 772–776.
864
865 Obrezkova, M.S., Kolesnik, A.N., Semiletov, I.P., 2014. The diatom distribution in the surface
866 sediments of the Eastern Arctic Seas of Russia. Russian Journal of Marine Biology, 40, 465–
867 472.
868
869 O'Brien, M.C., Macdonald, R.W. Melling, H., Iseki, K., 2006. Particle fluxes and geochemistry
870 on the Canadian Beaufort Shelf: Implications for sediment transport and deposition.
871 Continental Shelf Research, 26, 41–81.
872
873 O'Brien, M.C., Melling, H., Pedersen, T.F., Macdonald, R.W., 2011. The role of eddies and
874 energetic ocean phenomena in the transport of sediment from shelf to basin in the Arctic.
875 Journal of Geophysical Research, 116, C08001, doi:10.1029/2010JC006890.
876
877 Onodera, J., Takahashi, K., 2009. Long-term diatom fluxes in response to oceanographic
878 conditions at Stations AB and SA in the central subarctic Pacific and the Bering Sea, 1990–
879 1998. Deep-Sea Research I, 56, 189–211.
880
881 Onodera, J., Watanabe, E., Harada, N., Honda, M.C., 2015. Diatom flux reflects water-mass
882 conditions on the southern Northwind Abyssal Plain, Arctic Ocean. Biogeosciences, 12, 1373–
883 1385, doi:10.5194/bg-12-1373-2015.
884
885 Onodera, J.,Watanabe, E., Nishino, S., Harada, N., 2016. Distribution and vertical fluxes of
886 silicoflagellates, ebridians, and the endoskeletal dinoflagellate Actiniscus in the western Arctic
887 Ocean. Polar Biology, 39, 327–341, doi:10/1007/s00300-015-1784-y.
888

Poore, R.Z., Ishman, S.E., Phillips, L., McNeil, D., 1994. Quaternary stratigraphy and paleoceanography of the Canada Basin, western Arctic Ocean. US Geological Survey Bulletin, 2080, 1–32.

Post, E., Bhatt, U.S., Bitz, C.M., Brodie, J.F., Fulton, T.L., Hebblewhite, M., Kerby, J., Kutz, S., Stirling, I., Walker, D.A., 2013. Ecological consequences of sea‐ice decline. Science, 341, 519‐524.

Poulin, M., Lundholm, N., Bérard-Therriault, L., Starr, M., Gagnon, R., 2010. Morphological and phylogenetic comparisons of Neodenticula seminae (Bacillariophyta) populations between the subarctic Pacific and the Gulf of St. Lawrence. European Journal of Phycology, 45, 127-142.

Poulin, M., Daugbjerg, N., Gradinger, R., Ilyash, L., Ratkova, T., von Quillfeldt, C., 2011. The pan-Arctic biodiversity of marine pelagic and sea-ice unicellular eukaryotes: a first-attempt assessment. Marine Biodiversity, 41, 13–28.

Proshutinsky, A., Johnson, M., 1997. Two circulation regimes of the wind-driven Arctic Ocean. Journal of Geophysical Research, 102, 12 493–12 514.

Proshutinsky, A, Polyakov, I, Johnson, M., 1999. Climate states and variability of Arctic ice and water dynamics during 1946–1997. Polar Ressearch, 18, 135–142.

Proshutinsky, A., Dukhovskoy, D., Timmermans, M.-L., Krishfield, R., Bamber, J. L., 2015. Arctic circulation regimes. Philosophical Transactions of the Royal Society A, 373, 20140160.

Rabe, B., Karcher, M., Kauker, F., Schauer, U., Toole, J. M., Krishfield, R. A., Pisarev, S., Kikuchi, T., Su, J., 2014. Arctic Ocean basin liquid freshwater storage trend 1992–2012. Geophysical Research Letters, 41, 961–968. https://doi.org/10.1002/2013GL058121.

Ran, L.H., Chen, J.F., Jin, H.Y., Li, H.L., Lu, Y., Wang, K., 2013. Diatom distribution of surface sediment in the Bering Sea and Chukchi Sea. Advance in Polar Science, 24, 106–112.

Reid, P.C., Johns, D.G., Edwards, M., Starr, M., Poulin, M., Snoeijs, P., 2007. A biological consequence of reducing Arctic ice cover: arrival of the Pacific diatom Neodenticula seminae in the North Atlantic for the first time in 800 000 years. Global Change Biology, 13, 1910–1921.

Ren, J., Jiang, H., Seidenkrantz, M.-S., Kuijpers, A., 2009. A diatom-based reconstruction of Early Holocene hydrographic and climatic change in a southwest Greenland fjord. Marine Micropaleontology, 70, 166–176.

Ren, J., Gersonde, R., Esper, O., Sancetta, C., 2014. Diatom distributions in northern North Pacific surface sediments and their relationship to modern environmental variables, Palaeogeography, Palaeoclimatology, Palaeoecology, 402, 81–103.

Renaut, S., Devred, E., Babin, M., 2018. Northward expansion and intensification of phytoplankton growth during the early ice-free season in Arctic. Geophysical Research Letters, 45, 10590–10598.

Rigor, I.G., Wallace, J.M., Colony, R.L., 2002. Response of sea ice to the Arctic oscillation. Journal of Climate, 15, 2648–2663.

Roach, A.T., Aagaard, K., Pease, C.H., Salo, S.A., Weingartner, T., Pavlov, V., Kulakov, M., 1995. Direct measurements of transport and water properties through the Bering Strait. Journal of Geophysical Research, 100(C9), 18443-18457.

Romero, O.E., Armand, L.K., 2010. Marine diatoms as indicators of modern changes in oceanographic conditions. In: Smol, J.P., Stoermer, E.F. (eds), The Diatoms: Applications for the Environmental and Earth Sciences. Cambridge University Press, Cambridge, pp. 373-400.

Rowland, S.J., Belt, S.T., Wraige, E.J., Massé, G., Roussakis, C., Robert, J.M., 2001. Effects of temperature on polyunsaturation in cytostatic lipids of Haslea ostrearia. Phytochemistry, 56, 597–602.

Różańska, M., Gosselin, M., Poulin, M., Wiktor, J., Michel, C., 2009. Influence of environmental factors on the development of bottom ice protist communities during the winter–spring transition. Marine Ecology Progress Series, 386, 43-59.

Rutgers van der Loeff, M.M., Meyer, R., Rudels, B., Rachor, E., 2002. Resuspension and particle transport in the Benthic Nepheloid layer in and near Fram Strait in relation to faunal abundances and 234Th depletion. Deep-Sea Research Part I, 49, 1941–1958.

Sancetta, C., 1982. Distribution of diatom species in surface sediments of the Bering and

Okhotsk seas. Micropaleontology, 28, 221–257.

Saha, S., Moorthi, S., Pan, H.-L., Wu, X., Wang, J., Nadiga, S., Tripp, P., Kistler, R., Woollen, J., Behringer, D., Liu, H., Stokes, D., Grumbine, R., Gayno, G., Wang, J., Hou, Y.-T., Chuang, H., Juang, H.-M. H., Sela, J., Iredell, M., Treadon, R., Kleist, D., Delst, P. V., Keyser, D., Derber, J., Ek, M., Meng, J., Wei, H., Yang, R., Lord, S., van den Dool, H., Kumar, A., Wang, W., Long, C., Chelliah, M, Xue, Y., Huang, B., Schemm, J-K., Ebisuzaki, W., Lin, R., Xie, P., Chen, M., Zhou, S., Higgins, W., Zou, C-Z., Liu, Q., Chen, Y., Han, Y., Cucurull, L., Reynolds, R. W., Rutledge, G., Goldberg, M., 2010. The NCEP Climate Forecast System Reanalysis. Bulletin of American Meteorological Society, 91, 1015–1057.

Saha, S., Moorthi, S., Wu, X., Wang, J., Nadiga, S., Tripp, P., Behringer, D., Hou, Y.-T., Chuang, H.-Y., Iredell, M., Ek, M., Meng, J., Yang, R., Mendez, M.P., van den Dool, H., Zhang, Q., Wang, W, Chen, M., Becker, E., 2014. The NCEP Climate Forecast System Version 2. Journal of Climate, 27, 2185-2208.

Serreze, M.C., Maslanik, J.A., Scambos, T.A., Fetterer, F., Stroeve, J., Knowles, K., Fowler, C., Drobot, S., Barry, R.G., Haran, T.M., 2003. A record minimum arctic sea ice extent and area in 2002. Geophysical Research Letters, 30, 1110. https://doi.org/10.1029/2002GL016406.

Serreze, M.C., Crawford, A.D., Stroeve, J.C., Barrett, A.P., Woodgate, R.A., 2016. Variability, trends, and predictability of seasonal sea ice retreat and advance in the Chukchi Sea. Journal of Geophysical Research: Oceans, 121, doi:10.1002/2016JC011977.

Schrader, H.J., Gersonde, R., 1978. Diatoms and silicoflagellates. In: Zachariasse,W.J., Riedel, W.R., Sanfilippo, A., Schmidt, R.R., Brolsma, M.J., Schrader, H.J., Gersonde, R., Drooger, M.M., Broekman, J.A. (Eds.), Micropaleontological Methods and Techniques — An Exercise on an Eight Metres Section of the lower Pliocene of Capo Rossello, Sicily. Utrecht micropaleontological bulletins, 17, pp. 129–176.

Sha, L., Jiang, H., Liu, Y., Zhao, M., Li, D., Chen, Z., Zhao, Y., 2015. Palaeo-sea-ice changes on the North Icelandic shelf during the last millennium: Evidence from diatom records. Science China-earth Sciences, 58, 962-970.

Sha, L., Jiang, H., Seidenkrantz, M.-S., Muscheler, R., Zhang, X., Knudsen, M.F., Olsen, J., Knudsen, K.L., Zhang, W., 2016. Solar forcing as an important trigger for West Greenland sea-ice variability over the last millennium. Quaternary Science Review, 131, 148–156.

Sha, L., Jiang, H., Seidenkrantz, M.-S., Li, D., Andresen, C.S., Knudsen, K.L., Liu, Y., Zhao, M., 2017. A record of Holocene sea-ice variability off West Greenland and its potential forcing factors. Palaeogeography, Palaeoclimatology, Palaeoecology, 475, 115–124.

Shannon, C.E., Weaver,W., 1949. The Mathematical Theory of Communication, University of Illinois Press, Urbana, 125 pp.

Shimada, K., Kamoshida, T., Itoh, M., Nishino, S., Carmack, E., McLaughlin, F., Zimmermann, S., Proshutinsky, A., 2006. Pacific Ocean inflow: influence on catastrophic reduction of sea ice cover in the Arctic Ocean. Geophysical Research Letters, 33, L08605. http://dx.doi.org/10.1029/2005GL025624.

Smik, L., Belt, S.T., 2017. Distributions of the Arctic sea ice biomarker proxy IP25 and two phytoplanktonic biomarkers in surface sediments from West Svalbard. Organic Geochemistry, 105, 39–41.

Smik, L., Cabedo-Sanz, P., Belt, S.T., 2016. Semi-quantitative estimates of paleo Arctic sea ice concentration based on source-specific highly branched isoprenoid alkenes: Afurther development of the PIP25 index. Organic Geochemistry, 92, 63–69.

Smol, J.P., Stoermer, E.F., 2010. Applications and uses of diatoms: prologue. In: Smol, J.P., Stoermer, E.F. (eds), The Diatoms: Applications for the Environmental and Earth Sciences. Cambridge University Press, Cambridge, pp. 3-7.

Starr, M., St-Amand., L, Bérard-Therriault, L., 2002. State of phytoplankton in the Estuary and Gulf of St. Lawrence during 2001. DFO Canadian Science Advisory Secretariat Research Document 2002/067, Quebec: Fisheries and Oceans Canada, 23p.

Steele, M., Morison, J., Ermold, W., Rigor, I., Ortmeyer, M., Shimada, K., 2004. Circulation of summer Pacific halocline water in the Arctic Ocean. Journal of Geophysical Research, 109, C02027, doi:10.1029/2003JC002009.

Stein, R., Fahl, K., Schreck, M., Knorr, G., Niessen, F., Forwick, M., Gebhardt, C., Jensen, L., Kaminski, M., Kopf, A., Matthiessen, J., Jokat, W., Lohmann, G., 2016. Evidence for ice-free summers in the late Miocene central Arctic Ocean. Nature Communications, 7, 1–13.

Stein, R., Fahl, K., Gierz, P., Niessen, F., Lohmann, G., 2017. Arctic Ocean sea ice coverduring the penultimate glacial and the last interglacial. Nature Communications, 8, 373.

Sukhanova, I.N., Flint, M.V., Pautova, L.A., Stockwell, D.A., Grebmeier, J.M., Sergeeva, V.M., 2009. Phytoplankton of the western Arctic in the spring and summer of 2002: Structure and seasonal changes. Deep-Sea Research Part II, 56, 1223–1236.

Suto, I., 2004. Fossil marine diatom resting spore morpho-genus Xanthiopyxis Ehrenberg in the North Pacific and Norwegian Sea. Paleontological Research, 8, 283–310.

Tokuhiro, K., Abe, Y., Matsuno, K., Onodera, J., Fujiwara, A., Harada, N., Hirawake, T., Yamaguchi, A., 2019. Seasonal phenology of four dominant copepods in the Pacific sector of the Arctic Ocean: Insights from statistical analyses of sediment trap data. Polar Science, 19, 94–111.

Tsoy, I.B., Obrezkova, M.S., 2017. Atlas of Diatom Algae and Silicoflagellates from Holocene Sediments of the Russian East Arctic Seas. POI FEB RAS, Vladivostok 146 p.

Vare, L.L., Massé, G., Gregory, T.R., Smart, C.W., Belt, S.T., 2009. Sea ice variations in the central Canadian Arctic Archipelago during the Holocene. Quaternary Science Review, 28, 1354–1366.

von Quillfeldt, C.H., 1997. Distribution of diatoms in the Northeast Water Polynya, Greenland. Journal of Marine Systems, 211-240.

von Quillfeldt, C.H., 2000. Common Diatom Species in Arctic Spring Blooms: Their Distribution and Abundance. Botanica Marina, 43, 499-516.

von Quillfeldt, C.H., Ambrose, W.G., Clough, L.M., 2003. High number of diatom species in first-year ice from the Chukchi Sea. Polar Biology, 26, 806-818.

Walsh, J.J., Dieterle, D.A., Mullerkarger, F.E., Aagaard, K., Roach, A.T., Whitledge, T.E., Stockwell, D., 1997. CO2 cycling in the coastal ocean. II. Seasonal organic loading of the Arctic Ocean from source waters in the Bering Sea. Continental Shelf Research, 17, 1-36.

Wang, J., Hu, H., Goes, J. I., Miksisolds, J. L., Mouw, C. B., D'sa, E. J., Gomes, H., Wang, D.R., Mizobata, K., Saitoh, S., Luo, L., 2013. A modeling study of seasonal variations of sea

ice and plankton in the Bering and Chukchi Seas during 2007-2008. Journal of Geophysical Research: Oceans, 118, 1520-1533.

Wang, Q., Wekerle, C., Danilov, S., Koldunov, N. V., Sidorenko, D., Sein, D., Rabe, B., Jung, T., 2018. Arctic Sea Ice Decline Significantly Contributed to the Unprecedented Liquid Freshwater Accumulation in the Beaufort Gyre of the Arctic Ocean. Geophysical Research Letters, 45, 4956-4964.

Wassmann, P., 2011. Arctic marine ecosystems in an era of rapid climate change. Progress in Oceanography, 90, 1–17.

Wassmann, P., Bauerfeind, E., Fortier, M., Fukuchi, M., Hargrave, B., Moran, B., Noji, T., Nöthig, E.-M., Olli, K., Peinert, R., Sasaki, H., and Shevchenko, V., 2004. Particulate organic carbon flux to the Arctic Ocean sea floor. In: Stein, R., Macdonald, R.W. (eds), The organic carbon cycle in the Arctic Ocean. Berlin, Springer, pp101–138.

Wassmann, P., Duarte, C.M., Agusti, S., Sejr, M.K., 2011. Footprints of climate change in the Arctic marine ecosystem. Global Change Biology, 17, 1235–1249.

Watanabe, E., Onodera, J., Harada, N., Honda, M.C., Kimoto, K., Kikuchi, T., Nishino, S., Matsuno, K., Yamaguchi, A., Ishida, A., Kishi, M.J., 2014. Enhanced role of eddies in the Arctic marine biological pump. Nature Communication, 5, 3950, doi:10.1038/ncomms4950.

Watanabe, E., Onodera, J., Harada, N., Aita, M.N., Ishida, A., Kishi, J., 2015.Wind-driven interannual variability of sea ice algal production in thewestern Arctic Chukchi Borderland. Biogeosciences, 12, 1–22. doi: 10.519/bg-12-1-2015.

Weckström, K., Massé, G., Collins, L. G., Hanhijärvi, S., Bouloubassi, I., Sicre, M., Seidenkrantz, M.-S., Schmidt, S., Andersen, T.J., Andersen, M.L., Hill, B., Kuijpers, A., 2013. Evaluation of the sea ice proxy IP25 against observational and diatom proxy data in the SW Labrador Sea. Quaternary Science Reviews, 79, 53-62.

Weingartner, T., Aagaard, K. Woodgate, R., Danielson, S. Sasaki, Y., Cavalieri, D., 2005. Circulation on the north central Chukchi Sea shelf. Deep Sea Research, Part II, 52, 3150–3174.

Woodgate, R.A., 2018. Increases in the Pacific inflow to the Arctic from 1990 to 2015, and insights into seasonal trends and driving mechanisms from year-round Bering Strait mooring

data. Progress in Oceanography, 160, 124-154, doi:10.1016/j.pocean.2017.12.007.

Woodgate, R.A., Aagaard, K., Weingartner, T.J., 2005a. Monthly temperature, salinity, and transport variability of the Bering Strait throughflow. Geophysical Research Letters, 32(4), L04601, doi:10.1029/2004GL021880.

Woodgate, R., Aagaard, K., Weingartner, T., 2005b. A year in the physical oceanography of the Chukchi Sea: Moored measurement from autumn 1990–1991. Deep Sea Research, Part II, 52, 3116–3149.

Woodgate, R. A., Weingratner, T., Lindsay, R., 2010. The 2007 Bering Strait oceanic heat flux and anomalous Arctic sea-ice retreat. Geophysical Research Letters, 37, L01602, doi:10.1029/2009GL041621.

Woodgate, R.A., Weingartner, T.J., Lindsay, R., 2012. Observed increases in Bering Strait oceanic fluxes from the Pacific to the Arctic from 2001 to 2011 and their impacts on the Arctic Ocean water column. Geophysical Research Letters, 39, 6, doi: 10.1029/2012gl054092.

Woodgate, R.A., Stafford, K.M., Prahl, F.G., 2015. A Synthesis of Year-Round Interdisciplinary Mooring Measurements in the Bering Strait (1990–2014) and the RUSALCA Years (2004–2011). Oceanography, 28, 46-67.

Xiao, X., Fahl, K., Müller, J., Stein, R., 2015. Sea-ice distribution in the modern Arctic Ocean: Biomarker records from trans-Arctic Ocean surface sediments. Geochimica et Cosmochimica Acta, 155, 16–29.

Yokoi, N., Matsuno, K., Ichinomiya, M., Yamaguchi, A., Nishino, S., Onodera, J., Kikuchi, T., 2016. Short-term changes in a microplankton community in the Chukchi Sea during autumn: consequences of a strong wind event. Biogeosciences, 13, 913-923.

Zernova, V.V., Nöthig, E.-M., Shevchenko, V.P., 2000. Vertical microalga flux in the Northern Laptev Sea (from the data collected by the yearlong sediment trap). Oceanology, 40, 801–808.

Zhang, H., 2009. The Scientific Report on the 3rd Chinese National Arctic Research Expedition. Ocean Express, Beijing, 225p (in Chinese)

Zhuang, Y., Jin, H., Li, H., Chen, J., Lin, L., Bai, Y., Ji, Z., Zhang, Y., Gu, F., 2016. Pacific

inflow control on phytoplankton community in the Eastern Chukchi Shelf during summer. Continental Shelf Research, 129, 23–32.

Zhuang, Y., Jin, H., Chen, J., Li, H., Ji, Z., Bai, Y., Zhang, T., 2018. Nutrient and phytoplankton dynamics driven by the Beaufort Gyre in the western Arctic Ocean during the period 2008–2014. Deep-Sea Research Part I, 137, 30–37.

Diatom composition and fluxes over the Northwind Ridge, western Arctic Ocean: impact of marine surface circulation and sea ice distribution

Jian Ren *et al.*

Figures captions

Figure 1. a) Location of Station DM (red circle) and surface currents in the study area (grey arrows). The white dash line represents the multi-year sea ice minimum for 1979-2017 (20% of sea ice concentration) (from Cavalieri et al., 1996). Two other sites for discussion are also presented (yellow circles). Currents system: PWI- Pacific Water Inflow; ACW-Alaska Coastal Water; AW-Anadyr Water; BSW-Bering Slope Water; BG-Beaufort Gyre; SCC-Siberia Coastal Current. Topography: NR-Northwind Ridge; NAP-Northwind Abyssal Plain; CR-Chukchi Rise; CAP-Chukchi Abyssal Plain; MR-Mendeleev Ridge. b) Location of the sediment traps discussed in the text. The red dot shows Station DM (this study), the yellow dots show the other sites from previous studies.

Figure 2. Time series of daily environment variables, diatoms and biogeochemical tracers measured in the sediment trap moored at Station DM from August 2008 to September 2009. a) Shortwave radiation (W m^{-2}); b) Sea ice concentration (%); c) Sea ice thickness (m); d) Snow thickness (cm). a-d) are derived from the National Centers for Environmental Prediction (NCEP)/Climate Forecast System Reanalysis (CFSR) 6-hourly dataset (Saha et al., 2010, 2014). e) Total mass flux in mg m^{-2} d^{-1} (dark bar; from Bai et al., 2019), lithogenic matter flux in mg m^{-2} d^{-1} (grey bar) and percent weight of lithogenic matter (brown line); f) Particulate organic carbon (POC) flux in mg m^{-2} d^{-1} (Bai et al., 2019); g) Campesterol and β-sitosterol flux in µg m^{-2} d^{-1} represented by orange and brown bars, respectively; h) Stacked flux of different diatom groups in 10^6 valves m^{-2} d^{-1} (see text). Note that the fluxes in e) and g) are not stacked.

Figure 3. a-i) Diatom fluxes (in 10^5 valves m^{-2} d^{-1}) and relative abundances (in %) of the main species and species groups (see text) and j) diatom species diversity (H-index). Main species of *Chaetoceros* RS group in green (a), sea ice group in blue (b-e), cold-water group in purple (f-g), cosmopolitan group in red (h) and coastal group in yellow (i).

Figure 4. Time series of environment data and fluxes measured at Station DM. a) Arctic Ocean Oscillation index (Proshutinsky et al., 2015) which indicates the strength of Beaufort Gyre; b) Transport in Sv of the Pacific water inflow (Woodgate et al., 2015; Woodgate 2018); c) Sea ice concentration in % (Saha et al., 2010, 2014); d) Total diatom flux in 10^6 valves m^{-2} d^{-1}; e) Total mass flux in mg m^{-2} d^{-1} (Bai et al., 2019).

Figure 5. Representation of the surface currents and sea ice conditions in the study area in July and August of 2008 and 2009. PWI: Pacific water inflow, BG: Beaufort Gyre. Blocked currents by sea ice are indicated by the dashed lines. Sea ice data were retrieved from Nimbus-7 SMMR and DMSP SSM/I-SSMIS Passive Microwave Data with a grid resolution of 25 × 25 km (Cavalieri et al., 1996).

Figure 6. a) Sea ice concentration (in %) and terrigenous related fluxes: b) Coastal diatom flux in 10^5 valves m^{-2} d^{-1}; c) *Chaetoceros* resting spore flux in 10^5 valves m^{-2} d^{-1}; d) Total flux of campesterol and β-sitosterol in µg m^{-2} d^{-1}; e) Lithogenic matter flux in mg m^{-2} d^{-1} (grey bars) and lithogenic matter in % weight (red line). g) Bulk organic C/N ratio is also shown (blue line; Bai et al., 2019) and compared to the Redfield ratio as a reference (grey dash line).

Figure 7. a) Fluxes of sea ice diatom in 10^5 valves m^{-2} d^{-1} and IP_{25} in ng m^{-2} d^{-1} (relative to the internal standard). The occurrence of sea ice diatoms that produces IP_{25} are indicated by squares. b) Correlation plot between sea ice diatom flux and IP_{25} flux ($r^2 = 0.64$; $p < 0.01$).

Diatom composition and fluxes over the Northwind Ridge, western Arctic Ocean: impact of marine surface circulation and sea ice distribution

Jian Ren *et al.*

Figures

Figure 1-7

Figure 1

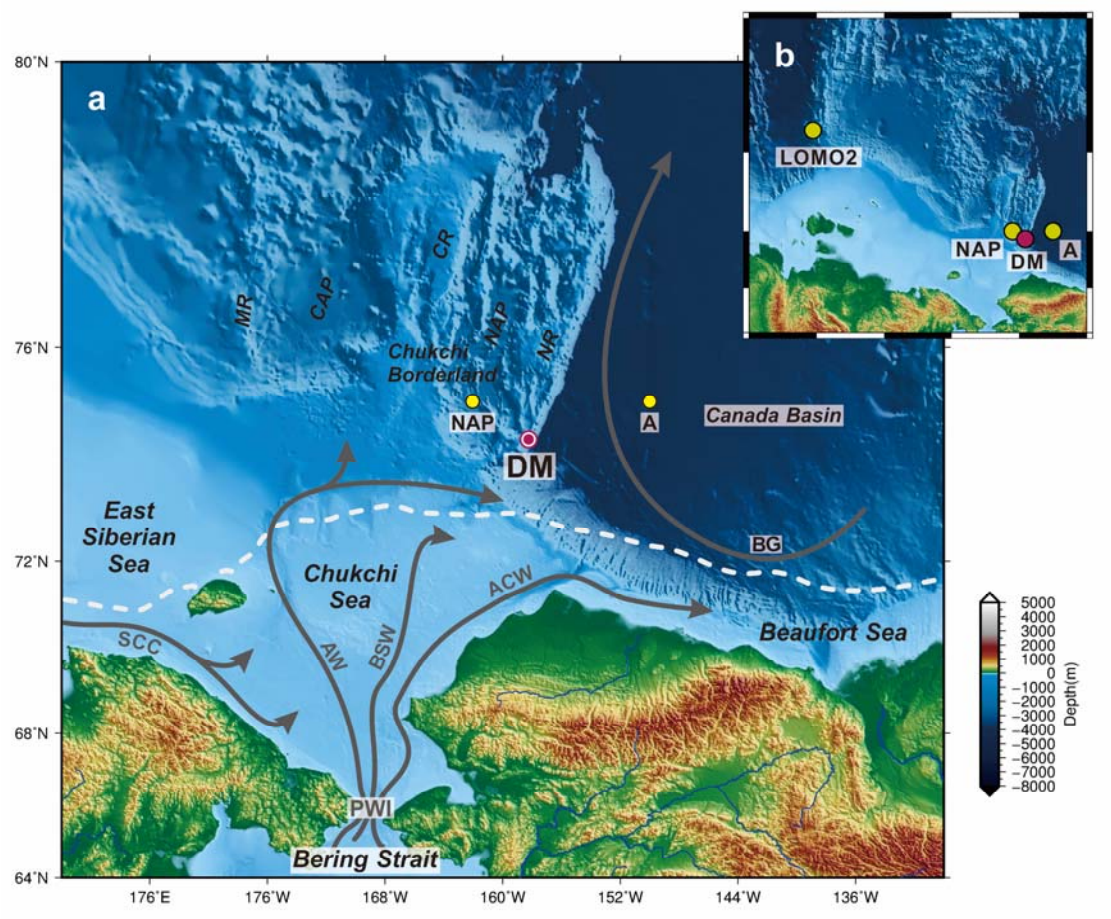
a
b
80°N
76°N
72°N
68°N
64°N
176°E
176°W
168°W
160°W
152°W
144°W
136°W
MR
CAP
CR
NAP
NR
Chukchi Borderland
NAP
DM
A
Canada Basin
East Siberian Sea
Chukchi Sea
BG
ACW
SCC
AW
BSW
PWI
Bering Strait
Beaufort Sea
LOMO2
NAP
DM
A
5000
4000
3000
2000
1000
0
−1000
−2000
−3000
−4000
−5000
−6000
−7000
−8000
Depth(m)

13 **Figure 2**

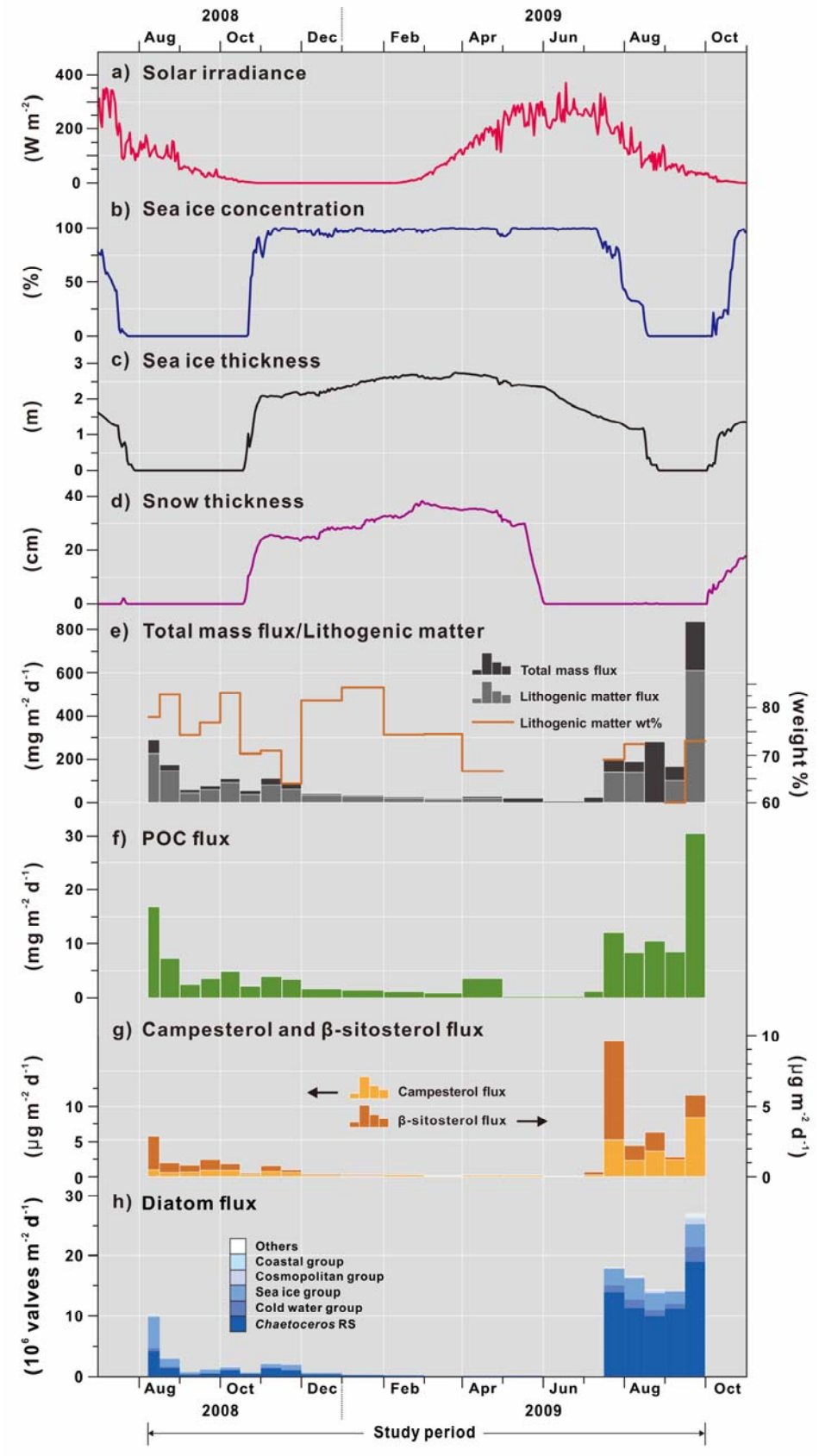
2008
2009
Aug
Oct
Dec
Feb
Apr
Jun
Aug
Oct
a) Solar irradiance
(W m-2)
b) Sea ice concentration
(%)
c) Sea ice thickness
(m)
d) Snow thickness
(cm)
e) Total mass flux/Lithogenic matter
(mg m-2 d-1)
Total mass flux
Lithogenic matter flux
Lithogenic matter wt%
(weight %)
f) POC flux
(mg m-2 d-1)
g) Campesterol and β-sitosterol flux
(μg m-2 d-1)
Campesterol flux
β-sitosterol flux
h) Diatom flux
(10^6 valves m-2 d-1)
Others
Coastal group
Cosmopolitan group
Sea ice group
Cold water group
Chaetoceros RS
Study period

14 **Figure 3**

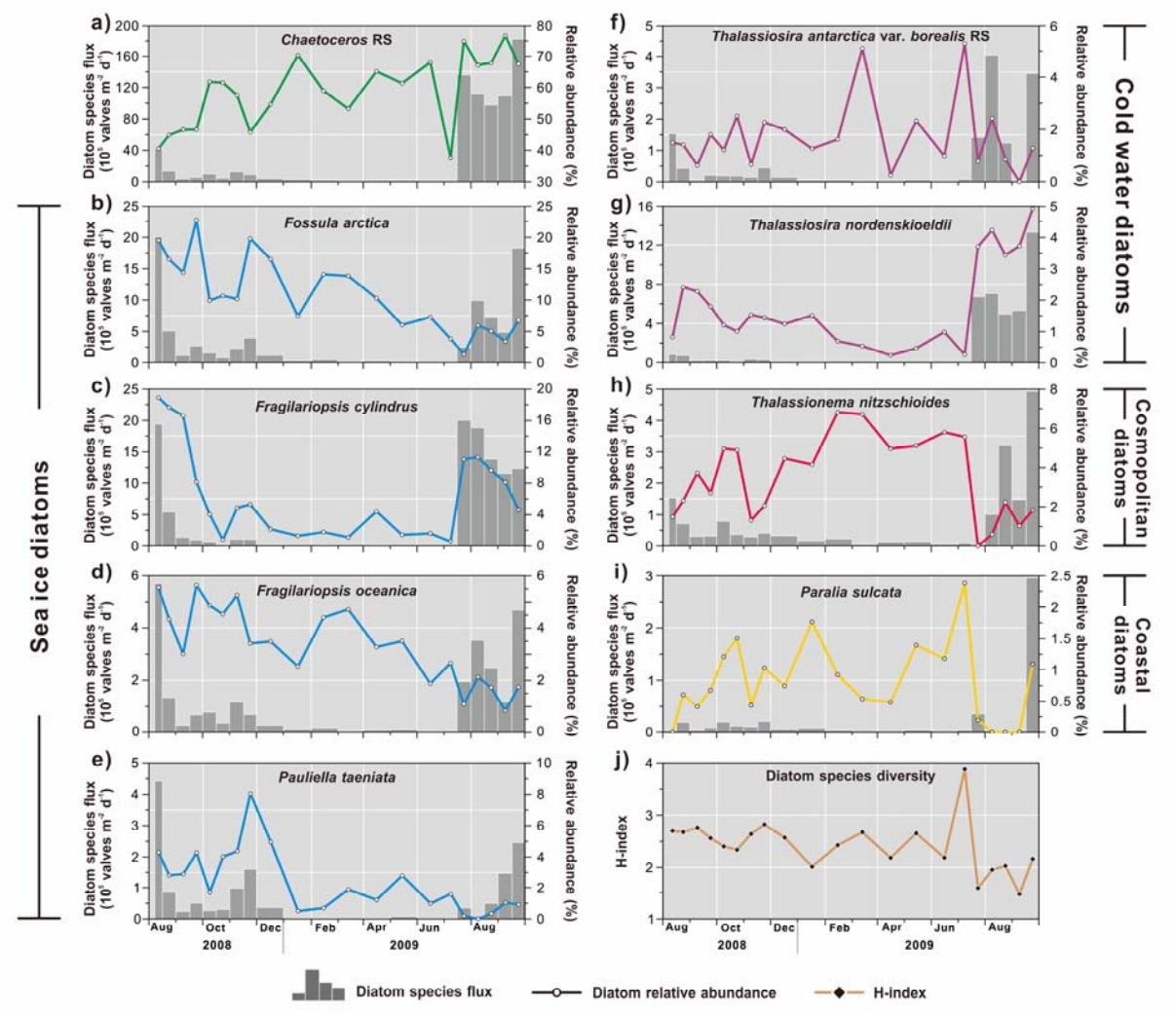
a) Chaetoceros RS
b) Fossula arctica
c) Fragilariopsis cylindrus
d) Fragilariopsis oceanica
e) Pauliella taeniata
f) Thalassiosira antarctica var. borealis RS
g) Thalassiosira nordenskioeldii
h) Thalassionema nitzschioides
i) Paralia sulcata
j) Diatom species diversity
Diatom species flux (10⁶ valves m⁻² d⁻¹)
Relative abundance (%)
H-index
Aug Oct Dec Feb Apr Jun Aug
2008
2009
Sea ice diatoms
Cold water diatoms
Cosmopolitan diatoms
Coastal diatoms
Diatom species flux
Diatom relative abundance
H-index

15 **Figure 4**

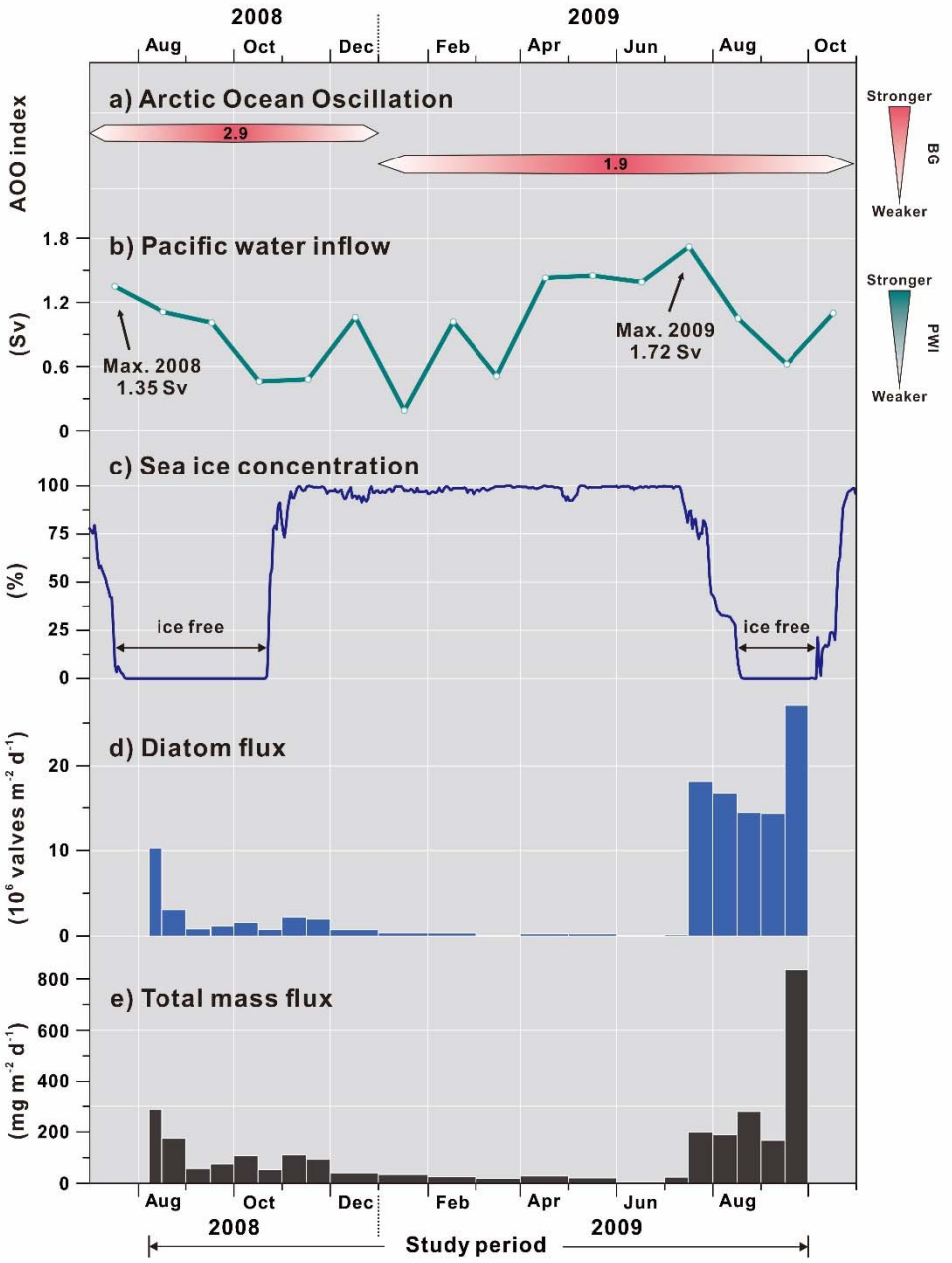
2008
2009
Aug
Oct
Dec
Feb
Apr
Jun
Aug
Oct
a) Arctic Ocean Oscillation
AOO index
2.9
1.9
Stronger
BG
Weaker
b) Pacific water inflow
(Sv)
1.8
1.2
0.6
0
Max. 2008
1.35 Sv
Max. 2009
1.72 Sv
Stronger
PWI
Weaker
c) Sea ice concentration
(%)
100
75
50
25
0
ice free
ice free
d) Diatom flux
(10^6 valves m^-2 d^-1)
20
10
0
e) Total mass flux
(mg m^-2 d^-1)
800
600
400
200
0
Aug
Oct
Dec
Feb
Apr
Jun
Aug
2008
Study period
2009

16 **Figure 5**

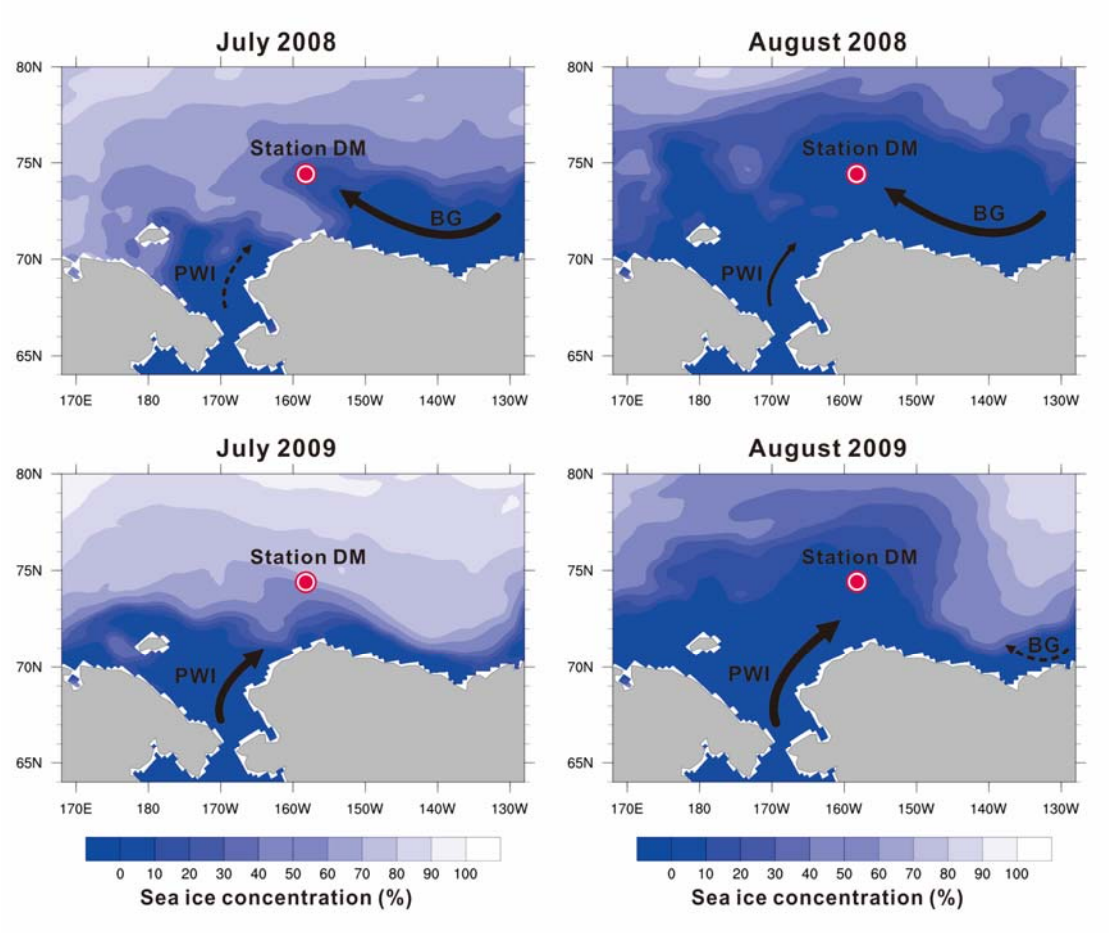
July 2008
August 2008
July 2009
August 2009
Station DM
BG
PWI
80N
75N
70N
65N
170E
180
170W
160W
150W
140W
130W
0 10 20 30 40 50 60 70 80 90 100
Sea ice concentration (%)

17 **Figure 6**

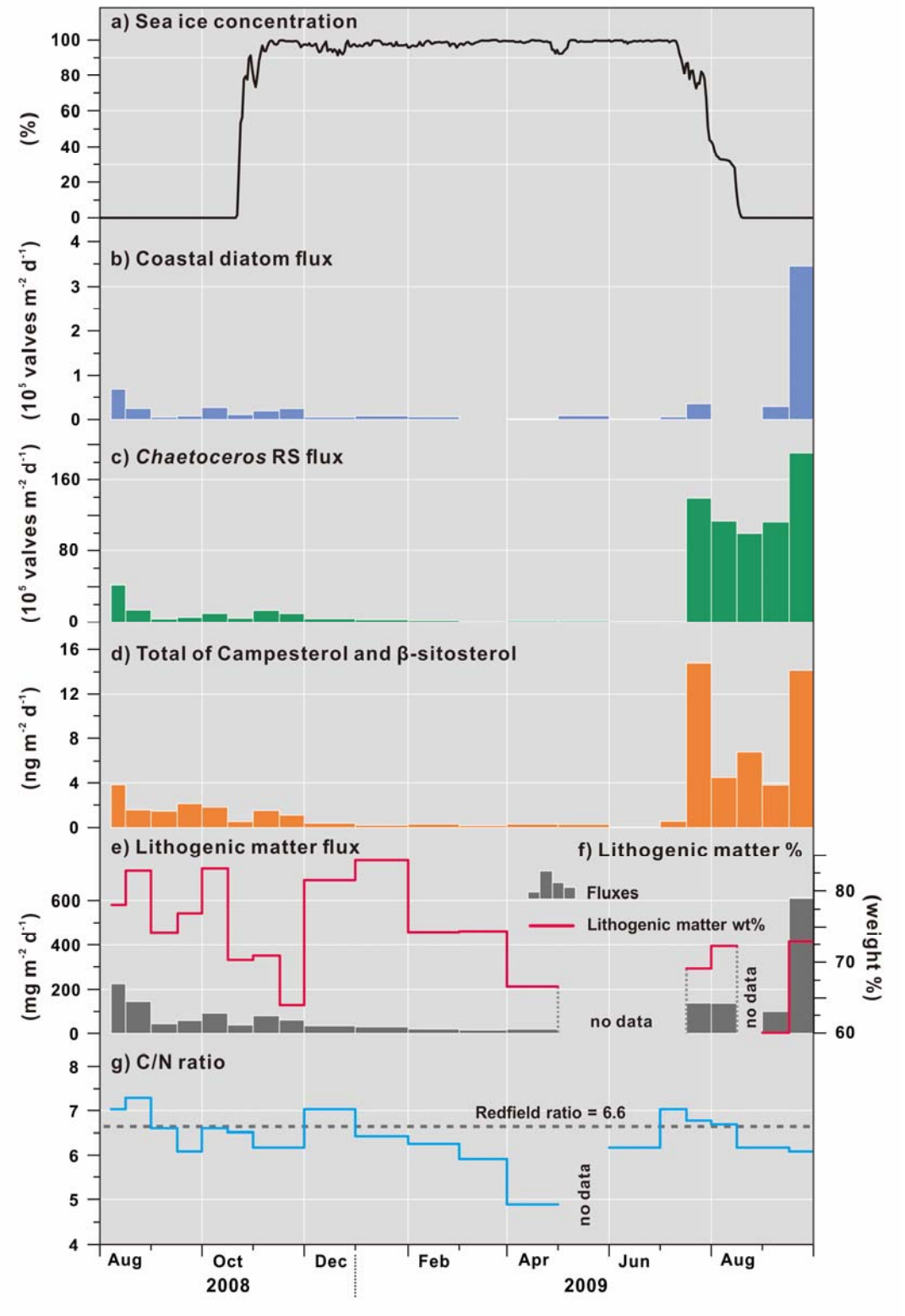
a) Sea ice concentration
(%)
b) Coastal diatom flux
(10⁵ valves m⁻² d⁻¹)
c) Chaetoceros RS flux
(10⁵ valves m⁻² d⁻¹)
d) Total of Campesterol and β-sitosterol
(ng m⁻² d⁻¹)
e) Lithogenic matter flux
(mg m⁻² d⁻¹)
f) Lithogenic matter %
Fluxes
Lithogenic matter wt%
(weight %)
no data
no data
g) C/N ratio
Redfield ratio = 6.6
no data
Aug
Oct
Dec
Feb
Apr
Jun
Aug
2008
2009

18 **Figure 7**

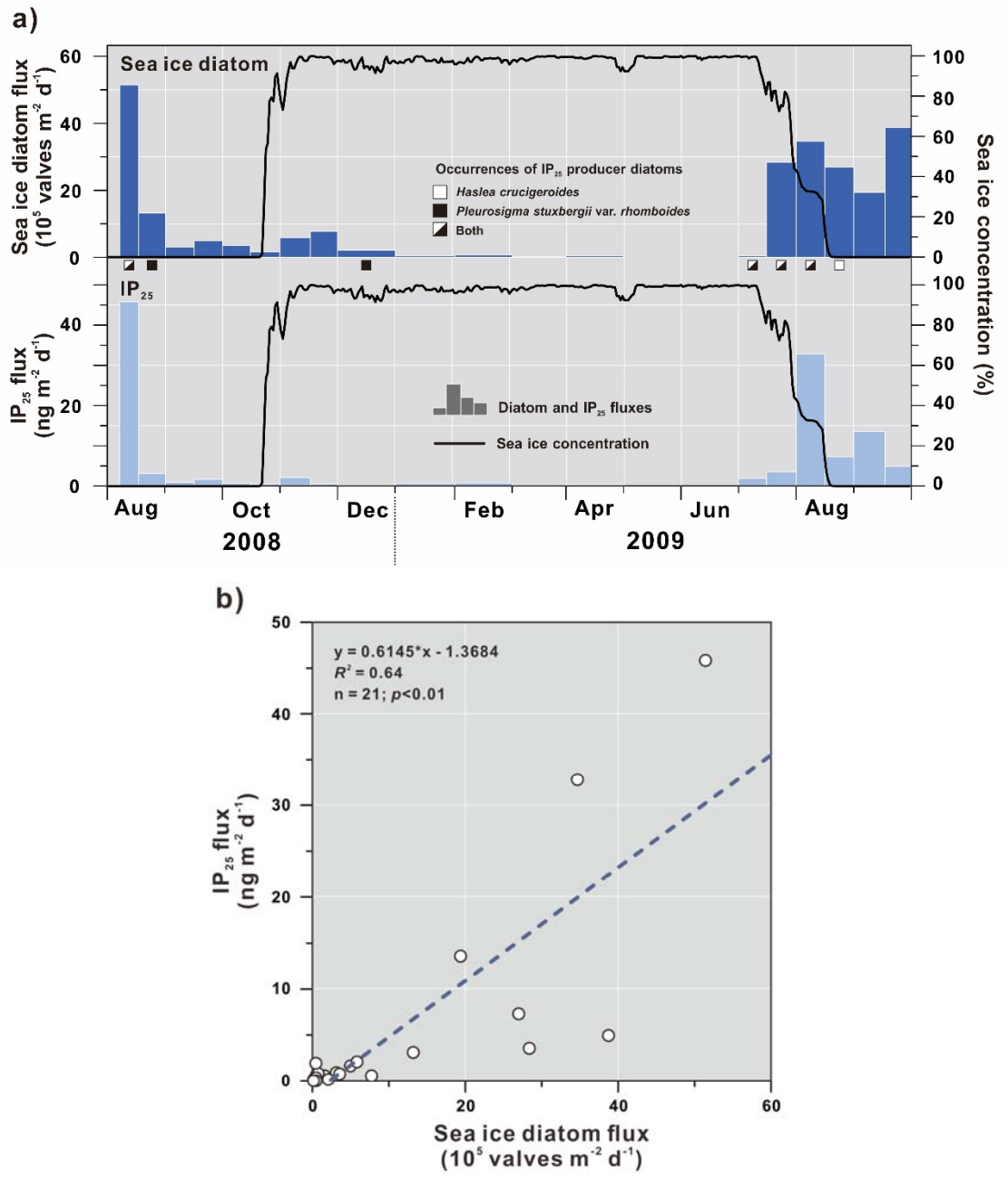
a)
Sea ice diatom
Sea ice diatom flux (10^5 valves m^-2 d^-1)
Occurrences of IP25 producer diatoms
Haslea crucigeroides
Pleurosigma stuxbergii var. rhomboides
Both
IP25
IP25 flux (ng m^-2 d^-1)
Diatom and IP25 fluxes
Sea ice concentration
Sea ice concentration (%)
Aug
Oct
Dec
Feb
Apr
Jun
Aug
2008
2009
b)
y = 0.6145*x - 1.3684
R^2 = 0.64
n = 21; p<0.01
IP25 flux (ng m^-2 d^-1)
Sea ice diatom flux (10^5 valves m^-2 d^-1)

Diatom composition and fluxes over the Northwind Ridge, western Arctic Ocean: impact of marine surface circulation and sea ice distribution

Jian Ren *et al.*

Supplementary Figure

Figure S1

Figure S1

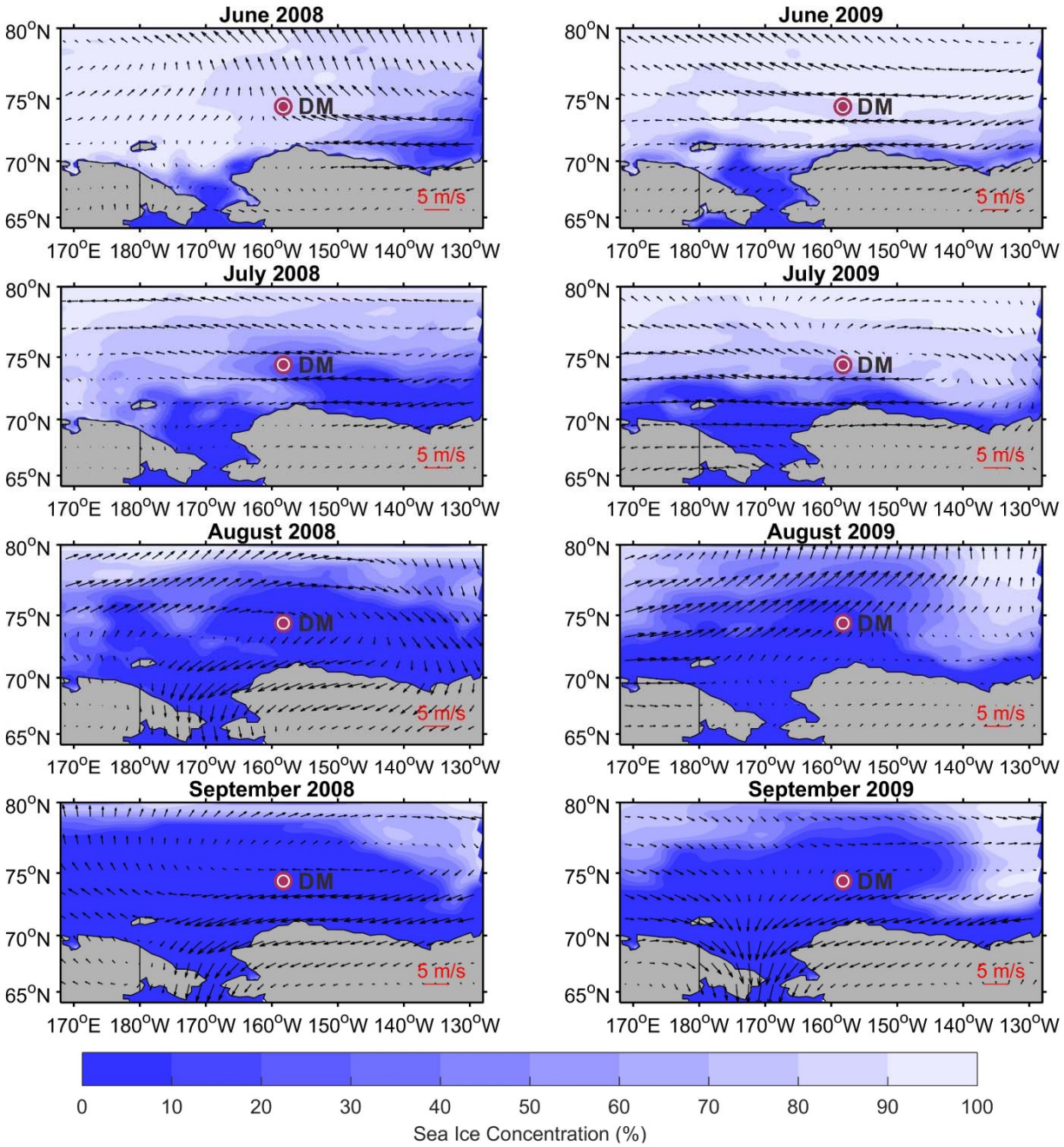

Figure S1. Wind field of the study area in June, July, August and September of 2008 and 2009. The wind data were retrieved from the NCEP/ NCAR atmospheric reanalysis data of daily 10 m-height wind speed (Kistler et al., 2001), with a horizontal resolution of 1.875°. Station DM and sea ice concentration are also shown.

Diatom composition and fluxes over the Northwind Ridge, western Arctic Ocean: impact of marine surface circulation and sea ice distribution

Jian Ren *et al.*

Table 1-2

Table 1

Table 1. Comparison of the diatom diversity and relative abundances from the sediment trap sinking particles at Station DM and nearby surface sediments

	Nr. of Species	H-index	*Chaetoceros* RS (%)	*Fossula arctica* (%)	*Fragilariopsis cylindrus* and *F. oceanica* (%)	*Thalassiosira nordenskioeldii* (%)	*Thalassiosira antarctica* var. *borealis* RS (%)
Station DM [a]	93	2.30	64.3 ± 11.3	8.2 ± 6.0	11.5 ± 6.0	2.9 ± 1.4	1.3 ± 1.4
Surface sediments [b]	78	2.46	63.3 ± 8.3	5.5 ± 2.9	11.3 ± 7.6	1.9 ± 1.1	3.3 ± 2.1

[a] Annual values based on merged seasonal samples

[b] Based on 10 surface sediments from northern Chukchi Sea (Ran et al., 2013)

Table 2

Table 2. Coefficient of determination (r^2) between fluxes and relative abundances (with and without *Chaetoceros* RS, respectively) of sea ice diatoms and cold water diatom group, fluxes of brassicasterol and dinosterol and fluxes of IP_{25} and HBI-III from August 2008 to September 2009 at Station DM. Significant correlations are shown in bold and underlined, while weak correlations are in bold and italic.

	Sea ice diatom flux[a]	**Cold-water diatom flux[a]**	**Sea ice diatom %**	**Cold-water diatom %**	**Sea ice diatom % (without *Chaetoceros* RS)**	**Cold-water diaotom % (without *Chaetoceros* RS)**	**Brassicasterol flux[b]**	**Dinosterol flux[b]**	**IP_{25} Flux[c]**	**HBI-III flux[c]**
Sea ice diatom flux[a]	1	-	-	-	-	-	-	-	-	-
Cold-water diatom flux[a]	**0.64***	1	-	-	-	-	-	-	-	-
Sea ice diatom %	0.02	0.09	1	-	-	-	-	-	-	-
Cold-water diatom %	0.02	0.09	0.002	1	-	-	-	-	-	-
Sea ice diatom % (without *Chaetoceros* RS)	0.11	0.01	**0.65***	0.05	1	-	-	-	-	-
Cold-water diatom % (without *Chaetoceros* RS)	0.14	***0.54****	0.43*	0.281**	0.21**	1	-	-	-	-
Brassicasterol flux[b]	0.44*	**0.83***	0.04	0.09	0.01	0.35*	1	-	-	-
Dinosterol flux[b]	***0.56****	**0.77***	0.06	0.05	0.002	0.45*	**0.67***	1	-	-
IP_{25} flux[c]	**0.64***	0.16	0.09	<0.0001	0.17	0.002	0.03	0.08	1	-
HBI-III flux[c]	***0.48****	0.03	0.24**	0.02	0.21**	0.06	0.01	0.02	**0.75***	1

[a] in 10^5 valves m^{-2} d^{-1}

[b] in µg m^{-2} d^{-1}

[c] in ng m^{-2} d^{-1}

* p-value < 0.01

** p-value < 0.05